# ANALYTICAL AND NUMERICAL ANALYSIS OF THE DISSIPATIVE KUNDU-ECKHAUS EQUATION

HAZAL YURTBAK

IŞIK UNIVERSITY
2019

# ANALYTICAL AND NUMERICAL ANALYSIS OF THE DISSIPATIVE KUNDU-ECKHAUS EQUATION

HAZAL YURTBAK

B.S., Mathematical Engineering, IŞIK UNIVERSITY, 2017

Submitted to the Graduate School of Science and Engineering
in partial fulfillment of the requirements for the degree of
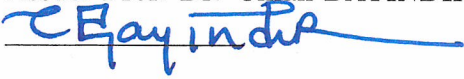Master of Science
in
Civil Engineering

IŞIK UNIVERSITY
2019

IŞIK UNIVERSITY
GRADUATE SCHOOL OF SCIENCE AND ENGINEERING

ANALYTICAL AND NUMERICAL ANALYSIS OF THE DISSIPATIVE
KUNDU-ECKHAUS EQUATION

HAZAL YURTBAK

APPROVED BY:

Assoc. Prof. Dr. Cihan BAYINDIR      İstanbul Technical University

Boğaziçi University

(Thesis Supervisor)

Prof. Dr. Hilmi DEMİRAY      Işık University

Prof. Dr. Nalan ANTAR      İstanbul Technical University

APPROVAL DATE:      02/12/2019

# ANALYTICAL AND NUMERICAL ANALYSIS OF THE DISSIPATIVE KUNDU-ECKHAUS EQUATION

## Abstract

It is well-known that the Kundu-Eckhaus equation (KEE) is a nonlinear equation which belongs to nonlinear Schrödinger class and it is commonly used as a model to investigate the dynamics of diverse phenomena in many areas including but are not limited to hydrodynamics, fiber and nonlinear optics, plasmas and finance. However, the effects of dissipation on the dynamics of KEE have not been investigated so far. In this thesis, in order to address this open problem we propose the dissipative Kundu-Eckhaus equation (dKEE) and perform an analytical and numerical analysis of the dKEE. With this motivation, we derive a simple monochromatic wave solution to dKEE. Then, we propose a split step Fourier method (SSFM) for the numerical solution of the dKEE and we test the stability of the SSFM using the analytical solution derived as a benchmark problem. Observing the stability and the accuracy of the scheme, we first investigate the rogue wave dynamics of the dKEE using the SSFM. More specifically, we show that modulation instability (MI) turns the monochromatic wave field into a chaotic one, thus the appearance of rogue waves become obvious. We discuss the properties and characteristics of such rogue waves. Additionally, we depict the amplitude probability distribution functions (PDFs) and discuss the effects of diffusion, Raman and dissipation coefficient as well as the MI parameters on the probability of rogue wave occurrence. Secondly, we investigate the effects of dissipation on the self-localized solitons of the KEE. For this purpose, we propose a Petviashvili method (PM) to obtain the self-localized solitons of the KEE and analyze the effects of dissipation by time stepping of these solitons using the SSFM proposed for dKEE. It is known that, KEE admits stable single, two and N-soliton solutions for the no potential case. It has been recently found that, under the effect of photorefractive and saturable potentials, such solitons of the KEE become unstable. We show that the dissipation parameter can be used to stabilize the single, two and three solitons of the KEE which do not satisfy the necessary Vakhitov-Kolokolov condition for the soliton stability. With this aim, we present the power graphs as functions of soliton eigenvalue and as well as time. Additionally, we depict the soliton shapes for various times to show that they are preserved for time scales long enough for many engineering purposes.

We comment on our findings and discuss the applicability and uses of our results. Additionally, we suggest possible directions for the near future research activities.

# SÖNÜMLÜ KUNDU-ECKHAUS DENKLEMİNİN ANALİTİK VE HESAPLAMALI ANALİZİ

## Özet

Kundu-Eckhaus denkleminin (KEE), doğrusal olmayan Schrödinger sınıfına ait bir denklem olduğu ve hidrodinamik, fiber ve doğrusal olmayan optik, plazma ve finans alanlarında bilinen ama bu alanlarla sınırlı kalmayan farklı olayların dinamiklerini araştırmak için yaygın olarak kullanılan bir model olduğu iyi bilinmektedir. Ancak KEE'nin dinamiği üzerinde sönümün etkileri araştırılmamıştır. Bu tezde, bu açık sorunu çözmek için, sönümlü Kundu-Eckhaus denklemi (dKEE) önerilmiş ve dKEE'nin analitik ve hesaplamalı çözümlerini ele alınmıştır. Bu motivasyon ile ilkin, dKEE için basit ve tek zamanlı bir dalga çözümü elde edilmiştir. Daha sonra dKEE'nin hesaplamalı çözümü için yarık basamaklama Fourier metodu (SSFM) önerilerek türetilen analitik çözüm test problemi olarak kullanılmış ve SSFM'nin hassasiyeti ve kararlılığı test edilmiştir. Şemanın hassasiyeti ve kararlılığı gözlendikten sonra, ilk önce dKEE'nin dev dalga dinamikleri SSFM kullanarak araştırılmıştır. Daha spesifik olarak, modülasyon kararsızlığının (MI) tek zamanlı dalga sahasını kaotik bir alana dönüştürdüğü gösterilmiş ve böylece dKEE bünyesinde dev dalgaların oluşabileceği gösterilmiştir. Ardından bu tür dev dalgaların özellikleri ve karakterleri tartışılmıştır. Ek olarak, dalga genlikleri için olasılık dağılım fonksiyonları (PDFs) üretilmiş ve difüzyon, Raman ve sönüm katsayısının yanı sıra ilgili MI parametrelerinin dev dalgaların ortaya çıkma olasılığı üzerine etkileri tartışılmıştır. İkincil olarak, sönümün KEE'nin öz yerel solitonlarının (tekil dalga) üzerine etkileri araştırılmıştır. Bu amaçla, KEE'nin öz yerel solitonlarını elde etmek için bir Petviashvili yöntemi (PM) önerilmiştir. Daha sonra PM ile elde edilen bu solitonlar SSFM kullanılarak zaman basamaklamaya tabi tutulmuştur. KEE'nin potansiyelsiz durumda kararlı tek, iki ve N-soliton çözümleri olduğu bilinmektedir. Son zamanlarda, fotorefraktif ve doyurulabilir potansiyellerin etkisi altında, KEE'nin bu tür solitonlarının dengesiz hale geldiği gösterilmiştir. Sönüm parametresinin, KEE'nin soliton dengesi için gerekli olan Vakhitov-Kolokolov koşulunu sağlamayan tekli, ikili ve üçlü solitonları dengelemek için kullanılabileceği gösterilmiştir. Bu amaçla, güç grafikleri soliton özdeğerinin ve zamanın birer fonksiyonu olarak sunulmuştur. Ek olarak, soliton şekilleri çeşitli zamanlarda oluşturulmuş ve birçok mühendislik amacı için yeterince uzun zaman ölçeklerinde korundukları gösterilmiştir. Sonuç

olarak, bu tezin bulguları hakkında yorumlar yapılmış ve sonuçların uygulanabilirliği, olası kullanım alanları ve yakın gelecekteki araştırma faaliyetleri için olası fikirler tartışılmıştır.

**Anahtar kelimeler:** Sönümlü Kundu-Eckhaus denklemi, doğrusal olmayan Schrödinger denklemi, spektral renormalleştirme metodu, zaman basamaklama Fourier metodu, dev dalgalar, modülasyon kararsızlığı

# Acknowledgements

# Table of Contents

# List of Figures

# List of Abbreviations

**1D**      **1 D**imension

**NLSE**    **N**onlinear **S**chrödinger **E**quation

**KEE**     **K**undu **E**ckhaus **E**quation

**dKEE**    **d**issipative **K**undu **E**ckhaus **E**quation

**MI**      **M**odulation **I**nstability

**PM**      **P**etviashvili **M**ethod

**SSFM**    **S**plit **S**tep **F**ourier Method

# Chapter 1

# Introduction

Nonlinear differential equations play a vital role in understanding vastly diverse phenomena in mathematics, physics, chemistry and other branches of applied sciences [1–5]. These diverse phenomena include but are not limited to fluid mechanics, solid-state physics, plasma physics, nonlinear optics, quantum mechanics, finance, atmospheric studies, celestial mechanics, biology, evolution etc [1,2,6–8]. One of the most commonly employed models in this fields is the nonlinear Schrödinger equation (NLSE) which was initially proposed by Schrödinger to describe the quantum state of an atomic particle. Later, it has been derived and employed for many different studies including but are not limited to water waves, plasmas, laser beams and electromagnetic transmission [9–20]. It is well-known that NLSE admit many different types of analytical solutions obtained by various techniques. These solutions include but are not limited to single, two, N-solitons solutions; rogue waves, rational solutions, chaoticons, kinks just to name a few [21–27]. The method employed for this purpose include but are not limited to brute force method, bilinear method, Darboux transforms, partial or discrete of the Painleve methods, Lax pairs, Bernoulli sub-equation method, exp-function method, gauge transformation, tangent-expansion method and extended auxiliary equation method [21, 24, 28–35]. The effects of dissipation on the dynamics and solutions of the NLSE have also attracted researchers' attention. In this context, the behavior of the dissipative NLSE in large-time is investigated in [36]. A new theory for the dissipative systems taking the velocity dependent frictional

forces into account in the frame of NLSE was studied in [37]. The phase-locked solitons with damped NLSE is analyzed in [38]. The slow manifold in a two-mode truncation of the damped forced NLSE is investigated in [39]. An analytical solution for the dissipative NLSE valid in the average sense was derived in [40]. Then, a numerical framework is proposed in [41] for the numerical solution of the dissipative NLSE.

The Eckhaus equation, on the other hand, is a nonlinear differential equation similar to the nonlinear Schrödinger equation(NLSE) in mathematics and physics. This equation was introduced by Kundu [4] and Eckhaus [5], independently. Therefore, this equation is more commonly known as Kundu-Eckhaus equation (KEE). KEE has two extension terms to the NLSE. The first extension term is the quintic nonlinearity term and the second one is the Raman effect term [4, 5, 41]. Similar to the NLSE, the KEE can be used to model various physical phenomena in nonlinear physics. These phenomena include but are not limited to nonlinear dispersive water waves, nonlinear optical waves, nonlinear processes in the quantum field theory, ion-acoustic waves, cosmic plasmas and various processes in finance [42–52]. Similar to the NLSE, the KEE admits many different type of solutions including but are not limited to single, two, N-solitons; rogue waves, kinks, rational solutions etc. [33, 45, 47–51, 53–58]. The methods utilized to derive such analytical solutions include but are not limited to brute force method, gauge and the Darboux transformations [45], Lie symmetry method [17], Bernoulli sub-equation function method [54], Laplace-Adomian decomposition method [55], Hamiltonian perturbation method [59], Miura transformation [3], similarity transformation method [60], Fokas method [56], extended trial equation method and extended $G'/G$ expansion scheme [61].

However, dissipative Kundu-Eckhaus equation (dKEE) has not been investigated so far.This thesis aims to address this open problem. With this motivation, in Chapter 2, we begin by deriving an analytical solution to the dKEE in the form of a monochromatic wave with time dependent amplitude and velocity. Later,

2

this analytical solution will serve as a benchmark problem for our numerical simulations.

In Chapter 3 of this thesis, we propose a numerical method to investigate the solutions of the dKEE with no potential. More specifically, for the time stepping of the dKEE we propose a split step Fourier method (SSFM). In this method that we propose with dKEE, the time stepping is handled by a first order time stepping and the spectral derivatives are computed using Fast Fourier transforms (FFTs). After checking the accuracy and the stability of this numerical scheme using the analytical solution of the dKEE presented in Chapter 2, we show that the rogue wave dynamics of the dKEE by can be studied by using SSFM proposed. It is well-known that when the sinusoidal solution of the NLSE like equations are subjected to noise, the modulation instability (MI) turns the monochromatic wave field into a chaotic one exhibiting unexpected large amplitude waves known as rogue waves [11–13] observed in diverse areas [62–66]. The SSFM proposed in Chapter 3 can be used to analyze such rogue waves of the dKEE as discussed in Chapter 5 of this thesis. Additionally, we propose a Petviashvili method (PM) to investigate the self-localized solitons of the dKEE with no potential.

In Chapter 4, we extend the mathematical framework proposed in Chapter 3 for the no potential case to account for the potential case. More specifically, we extend the SSFM and PM to account for the effects of the potential term. Although different potentials can be studied using this framework, we consider the case of a photorefractive potential and perform the extensions of the methodology accordingly.

In Chapter 5, we present a comprehensive discussion on our findings. Firstly, we discuss the dynamics and properties of rogue waves of the dKEE. We also discuss the effects of coefficients of the dKEE, the effects of MI and the effects of photorefractive potential term on the amplitude and rogue wave probability distributions. We show that all coefficients have an effect on these probabilities, however, the most dominant effect is the effect of dissipation. Although, the potential term

increases the probability of rogue wave occurrence, a small dissipation coefficient suppresses this effect by dissipating the waves in the chaotic field significantly. Secondly, we present an analysis on the self-localized solitons of the dKEE. We show that single, two and N-solitons of the KEE can be stabilized using an appropriate dissipation coefficient which guarantees that the solitons do not blow up and keep their soliton shapes for times scales long enough for many practical purposes.

In Chapter 6, we discuss the importance and possible uses of our findings as well as our methodology implemented for the dKEE. We propose possible extensions to our analysis and conclude.

# Chapter 2

# Analytical Aspects of the Dissipative Kundu-Eckhaus Equation

The dissipative Kundu-Eckhaus equation (dKEE) can be written by extending the KEE given in [4, 5] using a dissipation parameter as

$$i\frac{\partial U}{\partial t} + \mu_1\frac{\partial^2 U}{\partial \xi^2} + \mu_2\left|U\right|^2 U + i\mu_3 U + \mu_4^2\left|U\right|^4 U - 2\mu_4 i\left(\left|U\right|^2\right)_\xi U = 0, \qquad (2.1)$$

where $t$ is the time and $\xi$ is the space parameter. In here, $\mu_i$ $(i = 1, 2, 3, 4)$ are some real constant coefficients and $U(\xi, t)$ is the unknown function to be determined from the solution of the nonlinear equation. The parameter $\mu_1$ is the diffraction constant, the parameter $\mu_2$ is the cubic nonlinearity constant and the parameter $\mu_4$ is the quintic nonlinearity and Raman scattering constant. The parameter $\mu_3$ controls the dissipation or gain, depending on its sign [40]. Seeking a solution of Eq.(2.1) in the form

$$U(\xi, t) = a(t)\, e^{i[k\xi - \Omega(t)]} \qquad (2.2)$$

where $a(t)$ and $\Omega(t)$ are some unknown real functions of time $t$, one can obtain the expression

$$U = Ae^{-\mu_3 t}e^{i\left[k\xi - \mu_1 k^2 t - \frac{\mu_2}{2\mu_3}A^2 e^{-2\mu_3 t} - \frac{\mu_4^2 A^4}{4\mu_3}e^{-4\mu_3 t} + c\right]} \qquad (2.3)$$

In here, $A$ and $c$ are some constants referring to the amplitude and phase, respectively. This is the most fundamental harmonic solution of the dKEE. It is possible to construct higher order solutions starting from the seed solution given by Eq.(2.3) using Darboux transformation formalism. We use the analytical solution given in Eq.(2.3) as a benchmark problem for the numerical computations presented in the coming sections.

# Chapter 3

# Numerical Aspects of the Dissipative Kundu-Eckhaus Equation Under No Potential

## 3.1 Split-Step Fourier Method for the Dissipative Kundu-Eckhaus Equation Under No Potential

Split-Step Fourier Method (SSFM) is a numerical method used to solve partial differential equations like NLSE in numerical analysis [67]. SSFM can be used to model equations with constant or variable coefficients [68]. Some researchers have used this method for the studies in the field of optical fiber communications [69]. They analyzed the efficiencies of the SSFM in solving the NLSE with different step sizes [69, 70]. Some other researchers have developed the SSFM using the migration method [71]. In SSFMs, various order splittings are possible, such as the operator exponential scheme (OES) and the simplified operator exponential scheme (SOES) proposed for the numerical solution of the NLSE [72]. In order to develop a SSFM utilizing a first order splitting for the numerical solution of the dKEE we begin by rewriting it as

$$iU_t = -(\mu_2 \left|U\right|^2 + \mu_4^2 \left|U\right|^4 - 2i\mu_4(\left|U\right|^2)_\xi + i\mu_3)U \qquad (3.1)$$

which can be exactly solved as

$$\tilde{U}(\xi, t_0 + \Delta t) = e^{i(\mu_2|U_0|^2 + \mu_4^2|U_0|^4 - 2i\mu_4(|U_0|^2)_\xi + i\mu_3)\Delta t} \, U_0 \qquad (3.2)$$

where $U_0 = U(\xi, t_0)$ is the initial condition, $\Delta t$ is the time step. One can evaluate the spatial derivatives here using the Fourier series so that it is possible to write

$$\tilde{U}(\xi, t_0 + \Delta t) = e^{i\left(\mu_2|U_0|^2 + \mu_4^2|U_0|^4 - 2i\mu_4 F^{-1}\{ikF[|U_0|^2]\} + i\mu_3\right)\Delta t} U_0 \qquad (3.3)$$

where the Fourier transform of a function $f(\xi)$ is defined as

$$\widehat{f}(k) = F[f(\xi)] = \int_{-\infty}^{+\infty} f(\xi) \exp[-ik\xi]d\xi \qquad (3.4)$$

in which $k$ is the Fourier transform parameter. In here, $F$ and $F^{-1}$ denote the forward and inverse Fourier transforms, respectively. Additionally, the remaining part of the dKEE is linear can be given as

$$iU_t = -\mu_1 U_{\xi\xi} \qquad (3.5)$$

This part of the equation can be solved spectrally using the Fourier series as

$$U(\xi, t_0 + \Delta t) = F^{-1}\left[e^{-i\mu_1 k^2 \Delta t} F[\tilde{U}(\xi, t_0 + \Delta t)]\right] \qquad (3.6)$$

Lastly, one can combine the Eq.(3.3) and Eq.(3.6) to get the final form of the time stepping algorithm as

$$U(\xi, t_0 + \Delta t) = F^{-1}\left[e^{-i\mu_1 k^2 \Delta t} F[e^{i(\mu_2|U_0|^2 + \mu_4^2|U_0|^4 - 2i\mu_4 F^{-1}[ikF[|U_0|^2]] + i\mu_3)\Delta t} U_0]\right] \quad (3.7)$$

Starting from the initial condition $U_0$, the time stepping is performed using the Eq.(3.7) in order to obtain the numerical solution of the dKEE. In the coming results section of this thesis, we first check the accuracy and the stability of the SSFM by comparing it with the analytical solution given by Eq.(2.3) as a benchmark problem. Then, using the SSFM proposed, we investigate the rogue wave dynamics and the stability of the self-localized solutions of the dKEE.

## 3.2 Petviashvili Method for the Dissipative Kundu-Eckhaus Equation Under No Potential

One of the possible ways of finding the self-localized solitons of the nonlinear wave equations is to transform them into Fourier space and iterate until the solutions converge. Petviashvili's method is one of these Fourier domain methods [73]. Petviashvili's method was later improved by Ablowitz and Musslimani [74] and this improved method is known as the Spectral Renormalization method. This computational method plays an important role in nonlinear sciences for computing self-localized states or solution of nonlinear wave guides [74–76]. The fundamental idea of the PM is to transform the governing equation, i.e. NLSE like equation, into Fourier space to obtain a nonlinear non-local integral equation. This nonlinear non-local integral equation is then coupled to an algebraic equation [74, 77]. The iterations are continued unless the convergence of the algebraic equation is satisfied [74, 77]. For the details of applying PM to NLSE and a coupled system of NLSE, the reader is referred to [74]. In this section, we apply the PM to the dKEE to obtain its self-localized solutions when the effects of potential are neglected. The dKEE with no potential can be given as

$$ iU_t + \mu_1 U_{\xi\xi} + \mu_2 \left|U\right|^2 U + \mu_4^2 \left|U\right|^4 U - 2\mu_4 i \left(\left|U\right|^2\right)_\xi U + i\mu_3 U = 0 \qquad (3.8) $$

as discussed above. The dependent and independent parameters are as before. It is possible to rewrite the Eq. (3.8) as

$$ iU_t + \mu_1 U_{\xi\xi} + N(\left|U\right|^2)U = 0 \qquad (3.9) $$

where the nonlinear term becomes $N(\left|U\right|^2) = \mu_2 \left|U\right|^2 + \mu_4^2 \left|U\right|^4 - 2\mu_4 i \left(\left|U\right|^2\right)_\xi + i\mu_3$. Using the ansatz, $U(\xi, t) = \eta(\xi, \mu)\exp(i\mu t)$ where $\mu$ shows the soliton eigenvalue, the dKEE becomes

$$ -\mu\eta + \mu_1 \eta_{\xi\xi} + N(\left|\eta\right|^2)\eta = 0 \qquad (3.10) $$

9

Furthermore by 1D Fourier transforming the $\eta$ as

$$\widehat{\eta}(k) = F[\eta(\xi)] = \int_{-\infty}^{+\infty} \eta(\xi) \exp[-ik\xi]d\xi \qquad (3.11)$$

the spectral representation of the Eq. (3.10) becomes

$$\widehat{\eta}(k) = \frac{F\left[N(|\eta|^2 \eta)\right]}{\mu + \mu_1 |k|^2} \qquad (3.12)$$

The formula given by Eq. (3.12) can be applied iteratively to obtain the self-localized solutions of the dKEE. It is known that this iteration scheme may diverge or may tend to zero [74]. In order to overcome this problem, one can introduce a new variable in the form of $\widehat{\eta}(k) = \alpha\widehat{\phi}(k)$ which has the spectral representation given by $\widehat{\eta}(k) = \alpha\widehat{\phi}(k)$. Using these substitutions, Eq. (3.12) becomes

$$\widehat{\phi}(k) = \frac{F\left[N(|\alpha|^2 |\phi|^2)\phi\right]}{\mu + \mu_1 |k|^2} = R_\alpha[\widehat{\phi}(k)] \qquad (3.13)$$

and corresponding iteration scheme becomes

$$\widehat{\phi}_{j+1}(k) = \frac{F\left[N(|\alpha_j|^2 |\phi_j|^2)\phi_j\right]}{\mu + \mu_1 |k|^2} \qquad (3.14)$$

One can multiply both sides of Eq. (3.13) with the the complex conjugate of the term in the left-hand-side of Eq. (3.13), i.e. $\widehat{\phi}^*(k)$, and can obtain the total energy by integrating the multiplied the expression which eventually leads to

$$\int_{-\infty}^{+\infty} \left|\widehat{\phi}(k)\right|^2 dk = \int_{-\infty}^{+\infty} \widehat{\phi}^*(k)R_\alpha[\widehat{\phi}(k)]dk \qquad (3.15)$$

which is the normalization constraint. This energy constraint guarantees the scheme to converge to the self-localized solitons of the system under investigation. This procedure of obtaining self-localized solutions of a nonlinear system, which is applied to the dKEE in this thesis, is known as the PM which can applied to many different nonlinear systems [74, 78]. When a single Gaussian or multi-Gaussians are used as the initial conditions, the system given by Eq. (3.13) and

10

Eq. (3.14), can be applied iteratively to find the self-localized solitons. This system of equations is subjected to successive iterations until the parameter $\alpha$ converges. We investigate the effects of various parameters of the dKEE and PM on the properties and stabilities of the self-localized solitons in Chapter 5 of this thesis.

# Chapter 4

# Numerical Aspects of the Dissipative Kundu-Eckhaus Equation Under Photorefractive Potential

The dissipative Kundu-Eckhaus equation (dKEE) under the effect of a photorefractive potential, $V(\xi)$, can be written as

$$i\frac{\partial U}{\partial t} + \mu_1 \frac{\partial^2 U}{\partial \xi^2} + \mu_2 |U|^2 U + i\mu_3 U + \mu_4^2 |U|^4 U - 2\mu_4 i \left(|U|^2\right)_\xi U - V(\xi)U = 0, \quad (4.1)$$

where the parameters are as discussed in Chapter 2. In here, $V(\xi)$ refers to the potential term. In fiber optical communications and femto-laser studies, the most common choice for the potential is the photorefractive potential. The photorefractive potential can be formulated by the expression $V(\xi) = I_o \cos^2(\xi)$ where $I_o$ is a constant. It is important to note that the stability of the solutions of the dKEE, especially its self-localized solutions obtained by PM, may significantly depend on the value of $I_o$ as discussed in [78]. However, this parameter is selected as $I_0 = 2.5$ throughout this thesis. The form of the photorefractive potential with these parameters is given in Fig. (4.1).
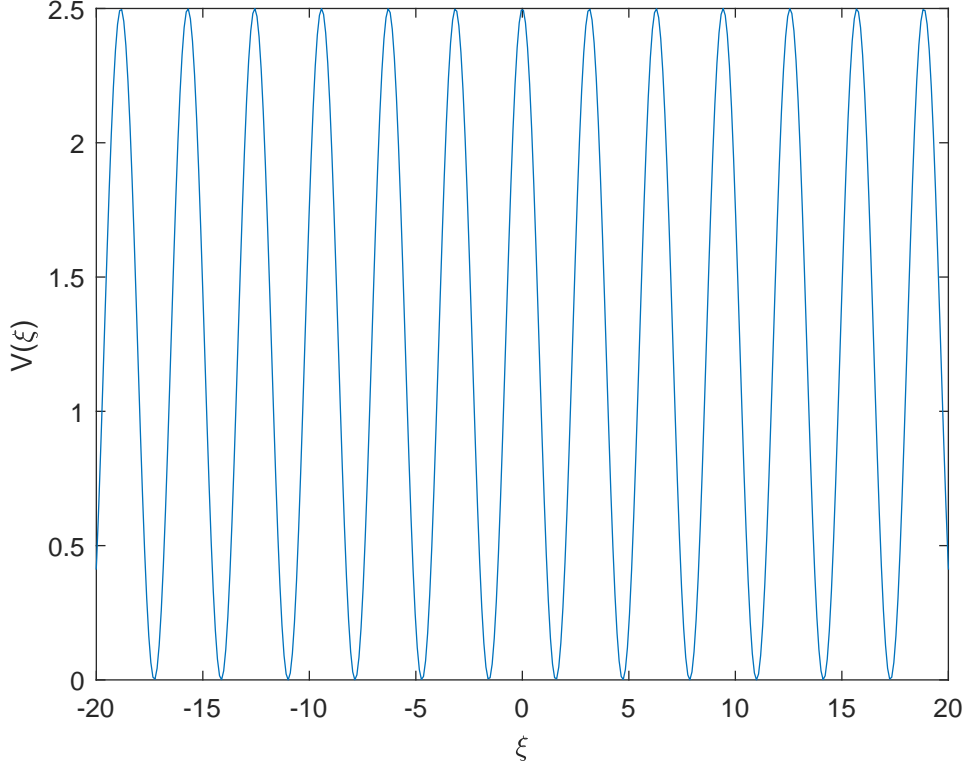
Figure 4.1: The photorefractive potential $V = I_o \cos^2(\xi)$ for $I_0 = 2.5$.

## 4.1 Split-Step Fourier Method for the Dissipative Kundu-Eckhaus Equation Under Photorefractive Potential

In here, we extend the SSFM discussed in Chapter 3.1 to account for the effects of the photorefractive potential. With this aim, we rewrite Eq. 4.1 as

$$iU_t = -(\mu_2 |U|^2 + \mu_4^2 |U|^4 - 2i\mu_4(|U|^2)_\xi + i\mu_3 - V(\xi))U \qquad (4.2)$$

which can be solved as

$$\tilde{U}(\xi, t_0 + \Delta t) = e^{i(\mu_2|U_0|^2 + \mu_4^2|U_0|^4 - 2i\mu_4(|U_0|^2)_\xi + i\mu_3 - V(\xi))\Delta t} U_0 \qquad (4.3)$$

where $U_0 = U(\xi, t_0)$ is the initial condition and $\Delta t$ is the time step, as discussed before in Chapter 3.1. Again, the spatial derivatives can be computed using the

13

Fourier series as

$$\tilde{U}(\xi, t_0 + \Delta t) = e^{i\left(\mu_2|U_0|^2 + \mu_4^2|U_0|^4 - 2i\mu_4 F^{-1}\{ikF[|U_0|^2]\} + i\mu_3 - V(\xi)\right)\Delta t} U_0 \qquad (4.4)$$

where $k$ shows the wavenumber parameter, and again $F$ and $F^{-1}$ denote the forward and inverse FFTs, respectively. Similar to before, the linear part of the dKEE becomes

$$iU_t = -\mu_1 U_{\xi\xi} \qquad (4.5)$$

which can be solved by utilizing the FFTs as

$$U(\xi, t_0 + \Delta t) = F^{-1}\left[e^{-i\mu_1 k^2 \Delta t} F[\tilde{U}(\xi, t_0 + \Delta t)]\right] \qquad (4.6)$$

Thus, the final form of the SSFM for the numerical solution of the dKEE can be obtained by combining Eq. (4.4) and Eq. (4.6), which leads to the expression

$$U(\xi, t_0 + \Delta t) = F^{-1}\left[e^{-i\mu_1 k^2 \Delta t} F[e^{i(\mu_2|U_0|^2 + \mu_4^2|U_0|^4 - 2i\mu_4 F^{-1}[ikF[|U_0|^2]] + i\mu_3 - V(\xi))\Delta t} U_0]\right]$$
$$(4.7)$$

We investigate the effect of the photorefractive potential on rogue wave formation probabilities and on the stability of the self-localized solutions of the dKEE using Eq. (4.7), as discussed in the Chapter 5 of this thesis.

## 4.2 Petviashvili Method for the Dissipative Kundu-Eckhaus Equation Under Photorefractive Potential

In this section of the thesis, we extend the PM proposed for dKEE in Chapter 3.2 to account for the effect of a potential term. For this scenario, the dKEE having a potential term becomes

$$iU_t + \mu_1 U_{\xi\xi} + \mu_2 |U|^2 U + \mu_4^2 |U|^4 U - 2\mu_4 i \left(|U|^2\right)_\xi U + i\mu_3 U - V(\xi)U = 0 \quad (4.8)$$

In here, the parameters are as discussed before in Chapter 3.2. Similarly, we consider a photorefractive potential given as $V(\xi) = I_o \cos^2(\xi)$, where $I_0 = 2.5$ as before. It is possible to rewrite the Eq. (4.8) as

$$iU_t + \mu_1 U_{\xi\xi} + N(|U|^2)U = 0 \tag{4.9}$$

where the nonlinear term is $N(|U|^2) = \mu_2 |U|^2 + \mu_4^2 |U|^4 - 2\mu_4 i \left(|U|^2\right)_\xi + i\mu_3 - V(\xi)$. Using the same ansatz as before, $U(\xi,t) = \eta(\xi,\mu)\exp(i\mu t)$ where $\mu$ shows the soliton eigenvalue, the dKEE with potential term becomes

$$-\mu\eta + \mu_1\eta_{\xi\xi} + N(|\eta|^2)\eta = 0 \tag{4.10}$$

The 1D Fourier transform of $\eta$, would give its spectral representation as

$$\widehat{\eta}(k) = F[\eta(\xi)] = \int_{-\infty}^{+\infty} \eta(\xi)\exp[-ik\xi]d\xi \tag{4.11}$$

Therefore, by taking the 1D Fourier transform Eq. (4.10), the iteration scheme for $\widehat{\eta}$ can be obtained. However, it is known that such an iteration scheme can turn out to be singular [74, 78]. In order to avoid such a singularity, one can add or subtract a $p\eta$ term with $p > 0$ to the 1D Fourier transform of Eq. (4.10). Throughout this thesis, a value of $p = 10$ is accepted. After these steps, one can obtain the iteration formula as

$$\widehat{\eta}(k) = \frac{(p + |\mu|)\widehat{\eta}}{p + \mu_1 |k|^2} - \frac{F[V\eta] - F\left[N(|\eta|^2)\eta\right]}{p + \mu_1 |k|^2} \tag{4.12}$$

where $V$ is the potential term. As before, the iterations of Eq. (4.12) may grow unboundedly or it may tend to zero [74]. Again, by introducing a new variable as $\eta(\zeta) = \alpha\phi(\xi)$ and its Fourier transform as $\widehat{\eta}(k) = \alpha\widehat{\phi}(k)$, helps us to overcome this problem. After these substitutions, Eq. (4.12) can be rewritten as

$$\widehat{\phi}(k) = \frac{F\left[N(|\alpha|^2 |\phi|^2)\phi\right]}{\mu + \mu_1 |k|^2} = R_\alpha[\widehat{\phi}(k)] \tag{4.13}$$

15

and corresponding iteration scheme becomes

$$\widehat{\phi}_{j+1}(k) = \frac{F\left[N(|\alpha_j|^2 |\phi_j|^2)\phi_j\right]}{\mu + \mu_1 |k|^2} \tag{4.14}$$

where $\alpha$ is used in an algebraic condition to check the convergence of the PM. This algebraic condition is basically an energy conservation principle. By multiplying the both sides of Eq. (4.14) with $\widehat{\phi}^*(k)$, where the sign $^*$ refers to complex conjugation, the total energy can be calculated as

$$\int_{-\infty}^{+\infty} \left|\widehat{\phi}(k)\right|^2 dk = \int_{-\infty}^{+\infty} \widehat{\phi}^*(k) R_\alpha[\widehat{\phi}(k)] dk \tag{4.15}$$

which is the normalization constraint of the PM algorithm. Starting from single or multi-Gaussians, the PM summarize above can be used to find the self-localized solitons of the dKEE with the potential term. We discuss the effects of various parameters of dKEE and PM as well as the photorefractive potential on existences, characteristics and stabilities on self-localized solitons in Chapter 5.

# Chapter 5

# Results and Discussion

In here, we present the numerical results for the dKEE obtained by the SSFM and PM. With this motivation, we first check the accuracy and stability of the SSFM using the analytical solution of the dKEE as a benchmark problem. In Chapter 5.1, we analyze the rogue wave fields generated in the frame of the dKEE and discuss the effects of dissipation on such fields. In Chapter 5.2 we investigate the effects of a photorefractive potential on the dynamics and statistics of rogue waves of the dKEE using the SSFM. Then, in Chapter 5.3 and in Chapter 5.4, we analyze the self-localized single, two and three soliton solutions of the dKEE with no and with photorefractive potential term, respectively. For this part of the analysis, we first utilize the PM to construct the self-localized soliton shapes, then we perform time stepping starting from these self-localized solitons using the SSFM. This procedure allows us to analyze the temporal dynamics and stabilities of such solitons, including the effects of dissipation.

## 5.1  Results and Discussion of the Rogue Wave Dynamics of the Dissipative Kundu-Eckhaus Equation

In Fig. (5.1), we compare the numerical solution of the dKEE and its analytical solution given by Eq. (2.3) at $t = 0$. For this simulation, the parameters of computation are selected as $\mu_1 = 1$, $\mu_2 = 2$, $\mu_3 = 0.1$ and $\mu_4 = 0.66$, $A = 0.2$. As

mentioned before, the number of spectral components is selected to be $N = 1024$ for this and other simulations presented in this thesis.



Figure 5.1: Comparison of the split-step vs exact solution of the dKEE at $t = 0.0$ for $\mu_1 = 1, \mu_2 = 2, \mu_3 = 0.1, \mu_4 = 0.66$ and $A = 0.2,$.
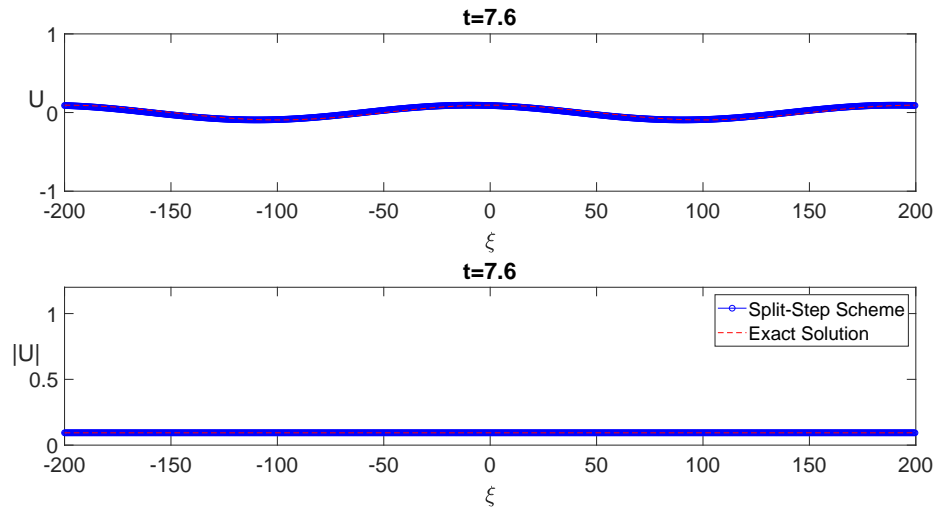


Figure 5.2: Comparison of the split-step vs exact solution of the dKEE at $t = 7.6$ for $\mu_1 = 1, \mu_2 = 2, \mu_3 = 0.1, \mu_4 = 0.66$ and $A = 0.2$.

In order to check the accuracy and stability of the SSFM, we perform the same comparison for $t = 7.6$ in Fig. (5.2). The time stepping is performed using a time step value of $\Delta t = 10^{-5}$ for all of our numerical simulations, as well as this one. As Fig. (5.2) confirms, the numerical solution is in good agreement with the

analytical solution, validating the accuracy and the stability of the SSFM scheme.
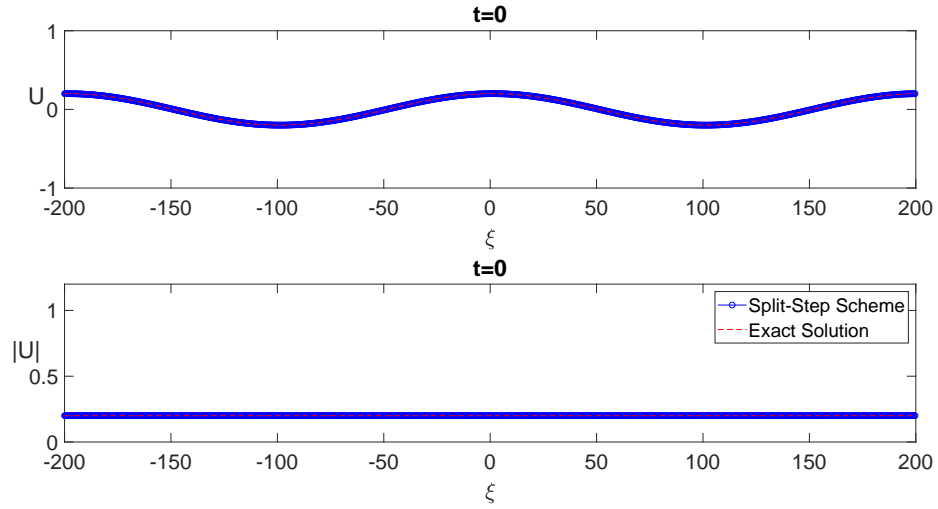


Figure 5.3: Comparison of the split-step vs exact solution of the dKEE at $t = 0.0$ for $\mu_1 = 1, \mu_2 = 2, \mu_3 = 1, \mu_4 = 0.66$ and $A = 0.2$.



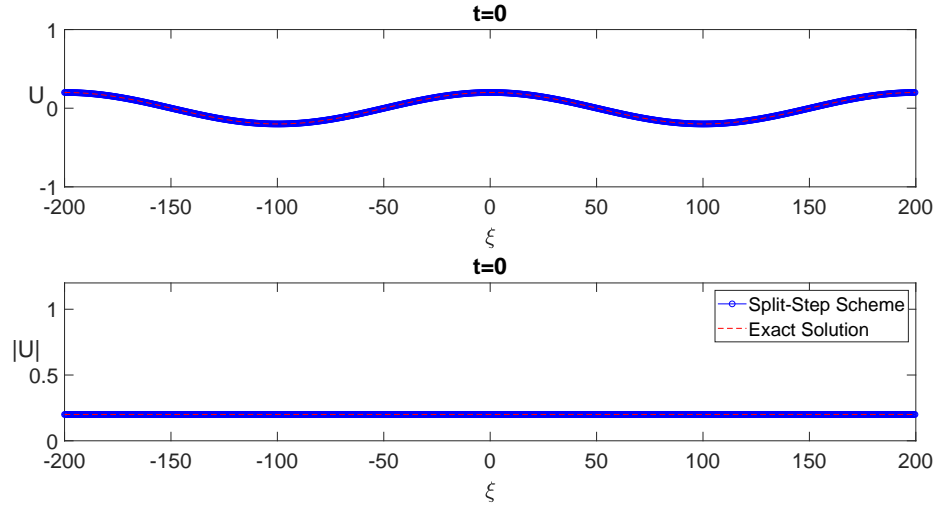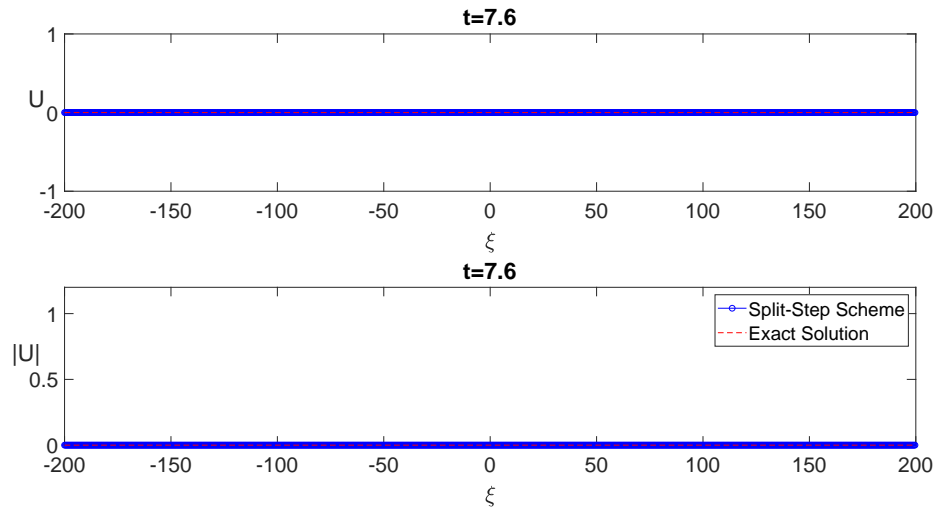Figure 5.4: Comparison of the split-step vs exact solution of the dKEE at $t = 7.6$ for $\mu_1 = 1, \mu_2 = 2, \mu_3 = 1, \mu_4 = 0.66$ and $A = 0.2$.

We repeat the similar simulations under the effect of stronger dissipation and plot the corresponding results in Fig. (5.3) and in Fig. (5.4) for $t = 0$ and $t = 7.6$, respectively. With this aim, we select the dissipation constant as $\mu_3 = 1$, and keep

the other parameters as before. As Fig. (5.3) and Fig. (5.4) confirm, the accuracy and stability of the SSFM is achieved, however, due to the larger dissipation coefficient the effects of the dissipation becomes more significant. This significant effect can be understood by realizing that the amplitude of the monochromatic wave vanishes at $t = 7.6$.

Next, we turn our attention to rogue wave dynamics of dKEE. For this purpose, we use the SSFM to analyze chaotic wave fields of the dKEE numerically. One of the possible mechanisms to excite such chaotic wave fields is the modulation instability (MI). It is well-known that MI can be triggered when an initial condition in the form of

$$U_0 = e^{imk_0\xi} + \beta a \tag{5.1}$$

is used in time stepping. In here, $U_0$ is the initial condition, $m$ is a constant, $k_0 = 2\pi/L$ is the fundamental wave number, $\beta$ is MI parameter and $a$ is a set of uniformly distributed random numbers which lie in the interval of $[-1, 1]$. The length of spatial domain is selected as $L = 400$ in the simulations presented in this thesis, and we zoom to wave profiles for better presentation purposes when it deems necessary.
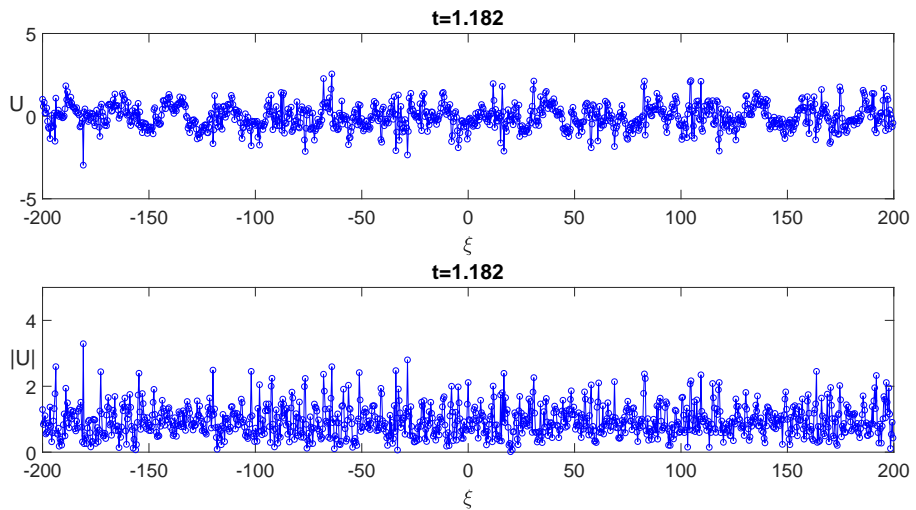


Figure 5.5: A typical chaotic wave field generated in the frame of dKEE for $\mu_1 = 1, \mu_2 = 2, \mu_3 = 0, \mu_4 = 0.66, m = 16$ and $\beta = 0.4$.

A typical chaotic wave field exhibiting rogue waves triggered by the MI in the frame of the dKEE is depicted in Fig. (5.5). The parameters of computation for this case is selected to be $\mu_1 = 1$, $\mu_2 = 2$, $\mu_3 = 0$, $\mu_4 = 0.66$, $m = 16$, $\beta = 0.4$, $A = 0.2$. During the time stepping we observed that majority of the wave amplitudes occur in the interval of $|U| \in [0, 5]$. These waves have very suddenly changing behavior in the chaotic wave fields, that is 'they appear from nowhere and disappear without a trace' [13, 47]. The waves having an amplitude of $|U| > 2$ can be classified as rogue waves, since we start our simulations using a sinusoid having a unit amplitude which is approximately the significant wave amplitude in the chaotic wave field.



Figure 5.6: Amplitude probability distribution for a chaotic wave field for $\mu_1 = 1, \mu_2 = 2, \mu_4 = 0.66$ for various values of $\mu_3$, $m = 4, \beta = 0.1$.

Next, we focus on the statistics of chaotic wave fields and rogue waves of dKEE. For this purpose, we perform massive numerical computations and plot the corresponding probability distribution functions (PDFs) of chaotic wave fields of dKEE in Figs. (5.6)-(5.10). After a dimensionless adjustment time of $t = 5$, the chaotic wave fields are recorded at 6 different times until $t = 10$. Each of these simulations performed for 10 realization. Thus, each of the PDFs presented in Figs. (5.6)-(5.10) include more than $6 \times 10^4$ waves. Checking Fig. (5.6), one can realize that dissipation constant of $\mu_3 = 0.1$ is strong enough to dissipate rogue

waves in the chaotic wave fields. We investigate the effect of MI parameter $\beta$



Figure 5.7: Amplitude probability distribution in a chaotic wave field for $\mu_1 = 1, \mu_2 = 2, \mu_4 = 0.66$ for various values of $\mu_3$, $m = 4$ and $\beta = 0.5$.

under the effect of dissipation in Fig. (5.7). It is well-known that an increase in $\beta$ results in an increase of the probability of rogue wave occurrence [47]. However, as Fig. (5.7) confirms under the effect of dissipation such an increase becomes indistinguishable.



Figure 5.8: Amplitude probability distribution in a chaotic wave field for $\mu_1 = 1, \mu_2 = 2, \mu_4 = 0.66$ for various values of $\mu_3$, $m = 16$ and $\beta = 0.1$.

Figure 5.9: Amplitude probability distribution in a chaotic wave field for $\mu_1 = 1, \mu_2 = 2, \mu_4 = 0.66$ for various values of $\mu_3, m = 16$ and $\beta = 0.5$.

It is also known that the parameter $m$ of Eq. (5.1) has an important effect on PDFs of amplitudes generally leading to an increase. Therefore, we perform similar simulations using the value of $m = 16$ for the cases of $\beta = 0.1$ and $\beta = 0.5$, and plot the resulting PDFs in Fig. (5.8) and Fig. (5.9), respectively. As before, the effect of dissipation turns out to be more significant compared to the effect of $m$.
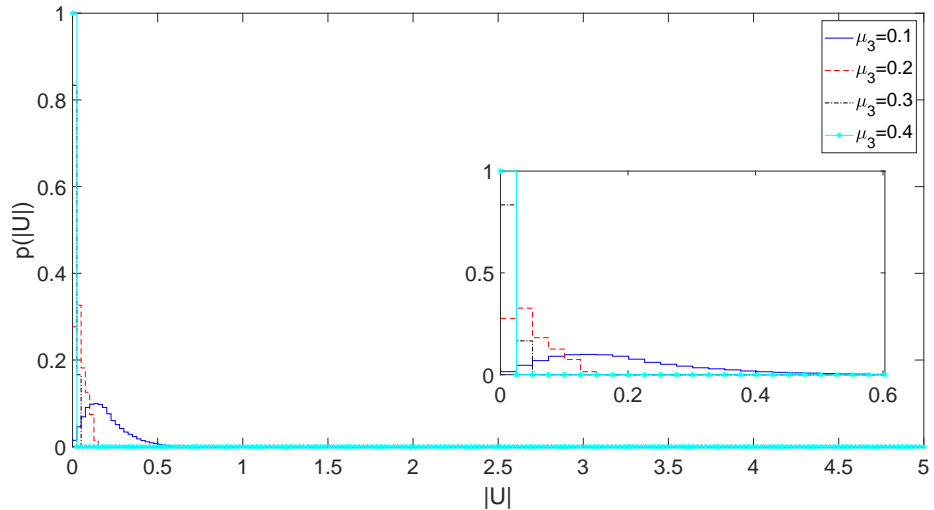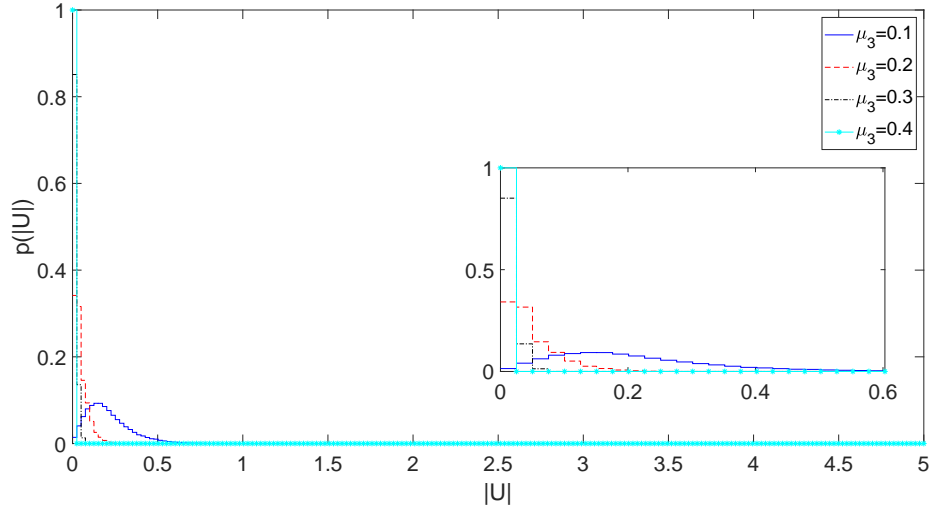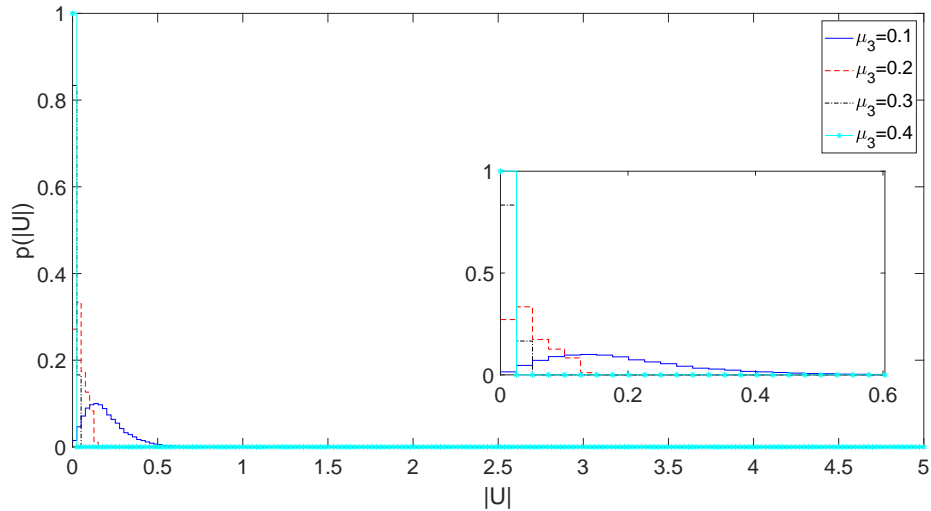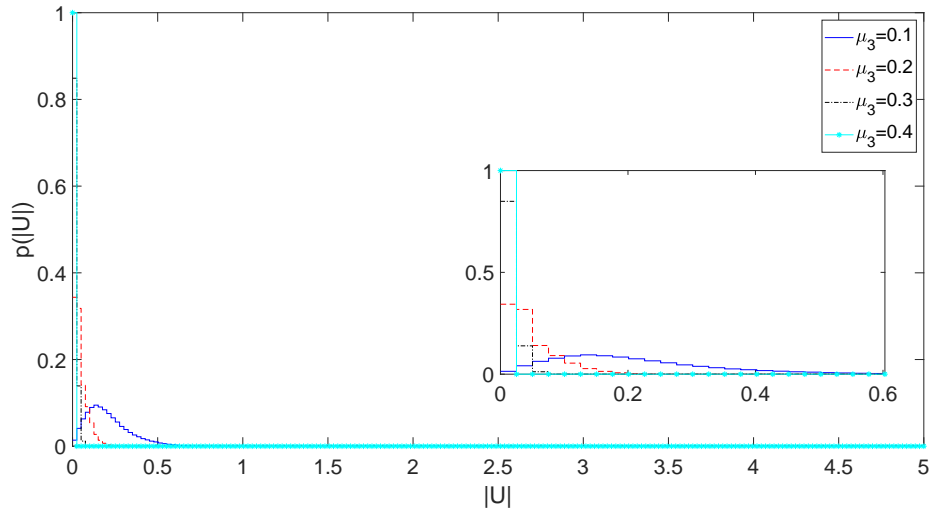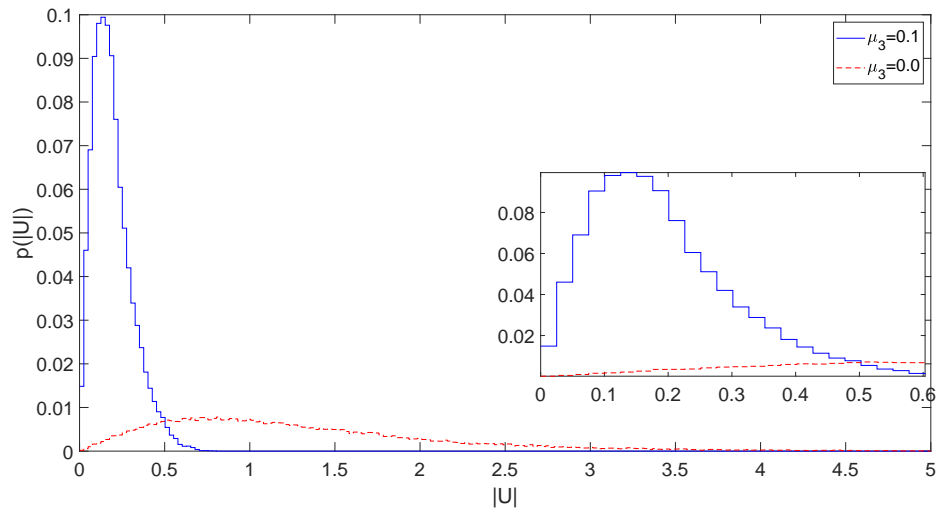


Figure 5.10: Amplitude probability distribution in a chaotic wave field for $\mu_1 = 1, \mu_2 = 2, \mu_4 = 0.66$ for $\mu_3 = 0.1$, $m = 4$, $\beta = 0.1$ and $\mu_3 = 0$.

23

Lastly, we compare the overall effect of the dissipation parameter, $\mu_3$, on the PDFs of wave amplitudes. With this motivation, we depict the red curve obtained for the non-dissipative case using $\mu_3 = 0$ and the blue curve obtained for the dissipative case using $\mu_3 = 0.1$ in Fig. (5.10). As it can be realized from the figure, even a small dissipation coefficient of $\mu_3 = 0.1$ has a significant effect on rogue wave formation. It is possible to argue that the amplitudes for which the probability is nonzero, lie in the interval of approximately $|U| \in [0, 4.5]$ for non-dissipative case, whereas the same interval reduces to $|U| \in [0, 0.75]$ for the dissipative case. This finding shows that even a small dissipation/gain coefficient can significantly change the probability of rogue wave occurrence when they are desired or not.

## 5.2 Results and Discussion of the Rogue Wave Dynamics of the Dissipative Kundu-Eckhaus Equation Under Photorefractive Potentials

In this section, we analyze the effect of photorefractive potential term on rogue waves of the dKEE. We perform the numerical simulations using the SSFM. Starting from the monochromatic wave superimposed with the white noise we perform the time stepping using Eq. (3.7) and Eq. (4.7) for the case of no and photorefractive potential, respectively. Using the same procedure of extracting rogue wave statistics as before, we depict the PDFs in Fig. (5.11).

The parameters of computation are selected to be $\mu_1 = 1, \mu_2 = 2, \mu_3 = 0, \mu_4 = 0.66, m = 4, \beta = 0.1$, the resulting statistics is depicted in Fig. (5.11). In this figure, the blue curve represents the PDF of amplitude distribution of the wave fields generated in the frame of dKEE when no potential term is considered. Whereas, the red curve represents the same PDF under the effect of the photorefractive potential. As Fig. (5.11) confirms, the photorefractive potential term leads to

Figure 5.11: Amplitude probability distribution in a chaotic wave field under photore-fractive potential for $\mu_1 = 1, \mu_2 = 2, \mu_3 = 0, \mu_4 = 0.66, m = 4$ and $\beta = 0.1$.

generation of larger amplitude waves in the frame of dKEE. One can easily recognize this fact by checking the probability increase for the amplitudes in the interval of approximately $|U| \in [1.7, 3.5]$.
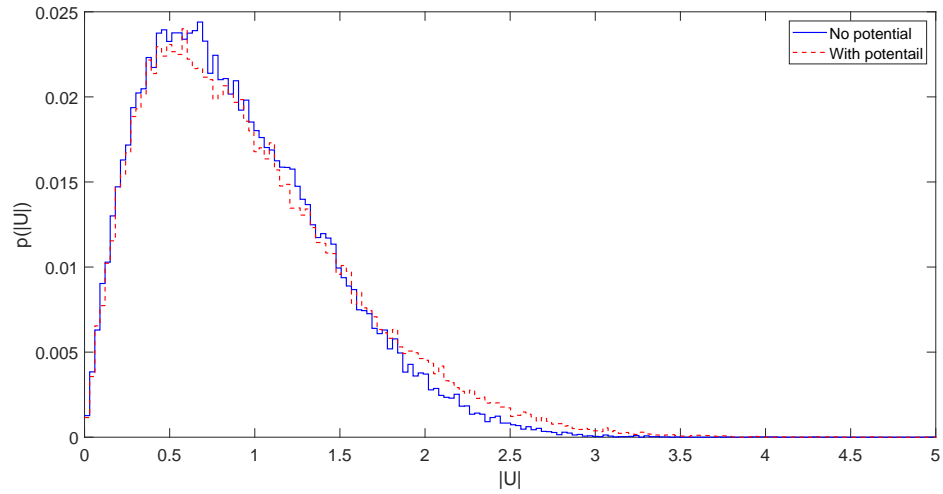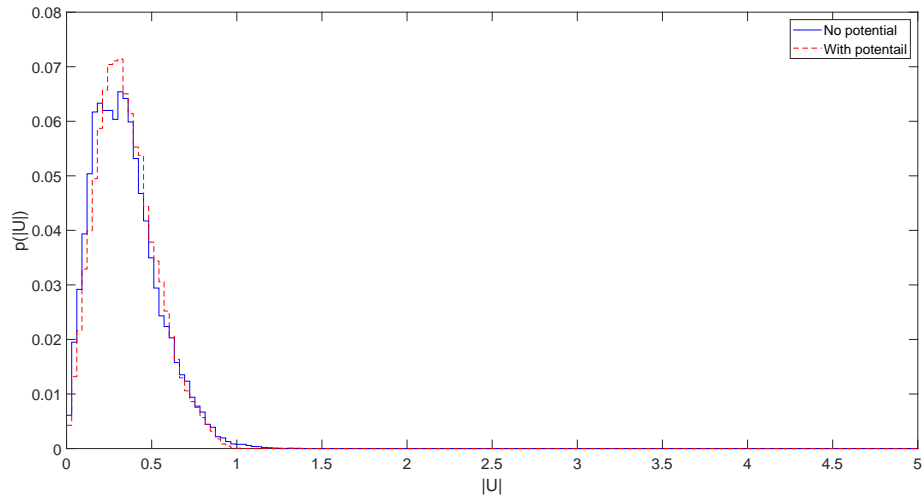


Figure 5.12: Amplitude probability distribution in a chaotic wave field under photore-fractive potential for $\mu_1 = 1, \mu_2 = 2, \mu_3 = 0.1, \mu_4 = 0.66, m = 4$ and $\beta = 0.1$.

In order to analyze the effect of such a potential under stronger dissipation, we repeat the same analysis using a dissipation parameter of $\mu_3 = 0.1$ and depict

the resulting PDFs in Fig. (5.12). In here we observe that the effect of dissipation becomes more dominant compared to the effect of photorefractive potential. However, after a careful checking of figure, we can argue that the potential term causes more waves in the interval of approximately $|U| \in [0.4, 0.7]$ to occur, resulting in a slight rightwards shift in the peak of the PDF. However due to higher dissipation, the effect of photorefractive potential becomes in distinguishable for the larger amplitudes of PDF.

## 5.3 Results and Discussion of the Self-Localized Solutions of the Dissipative Kundu-Eckhaus Equation Obtained by Petviashvili Method

In this section, we analyze the single, two and three self-localized solitons of the KEE under the effect of no potential term, $V = 0$. It is known that KEE with no potential admits single, two and N-soliton solutions [33,58]. For this purpose, we employ Eqs. (3.14) and (3.15) until the convergence of parameter $\alpha$ is achieved.

### 5.3.1 Single soliton

In this part, we discuss the properties of single self-localized soliton of the KEE. Starting from a simple Gaussian as initial condition, the PM rapidly converges to the single self-localized soliton. The convergence criteria is accepted as the normalized change of $\alpha$ to be less than $1 \times 10^{-10}$. The single soliton obtained by PM using this convergence criteria is depicted and compared with the analytical solution given by Eq.(3.13) in [33] for $\mu = 1$ in Fig. (5.13). As this figure confirms, the soliton shape can be constructed using PM and turns out to be in agreement with the analytical solution.

The self-localized soliton obtained by PM for various values of $\mu_1$ ($\mu_1 = 0.5, 1.0, 1.5,$ 2.0) is depicted in Fig. (5.14) and the direction of increase of $\mu_1$ is shown there. As one can see in Fig. (5.14), the self-localized single soliton of the KEE widens and its peak value decreases as $\mu_1$ increase.
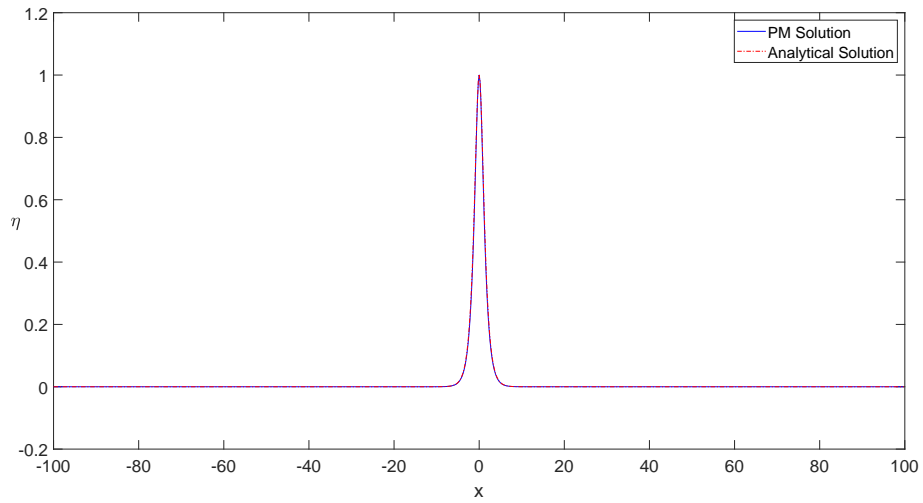
Figure 5.13: Comparison of the numerical solution obtained by PM with the analytical solution given by Eq.(3.13) in [33] for $\mu = 1$.
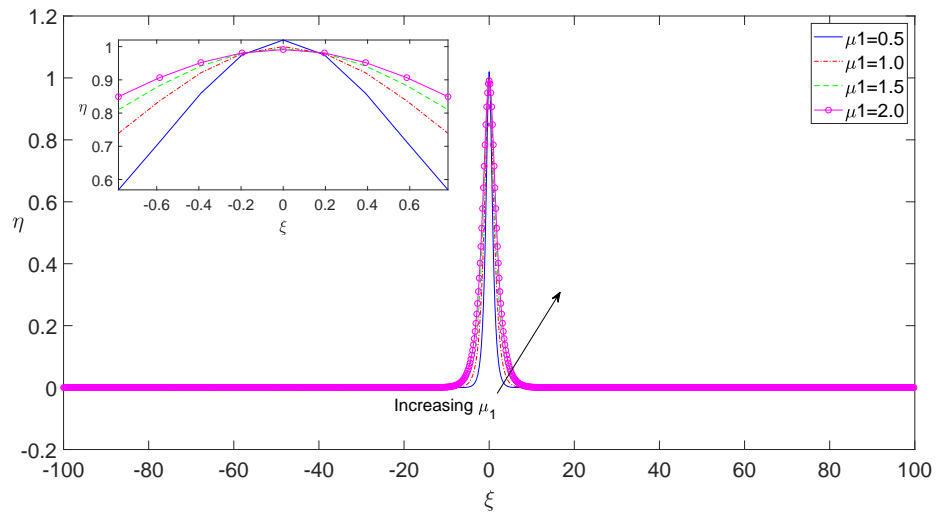


Figure 5.14: Self-localized single soliton solution as a function of $\xi$ for various $\mu_1$ values.

In Fig. (5.15) and Fig. (5.16), self-localized single solitons of the KEE obtained in a similar fashion is depicted for various values of $\mu_2$ and $\mu_4$, respectively. The values used in Fig. (5.15) for the $\mu_2$ parameter are taken as $\mu_2 = 1, 2, 3, 4, 5$. As indicated in Fig. (5.15) the self-localized single soliton of the KEE gets narrower and it is peak value decreases due to stronger diffusion. Similarly, as indicated in Fig. (5.16), the self-localized single soliton of the KEE gets narrower, however its
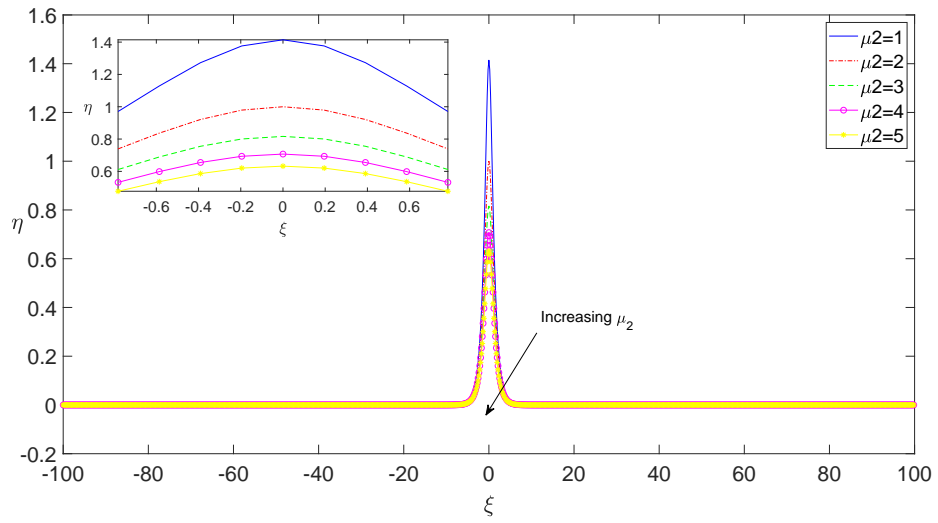
Figure 5.15: Self-localized single soliton solution as a function of $\xi$ for various $\mu_2$ values.
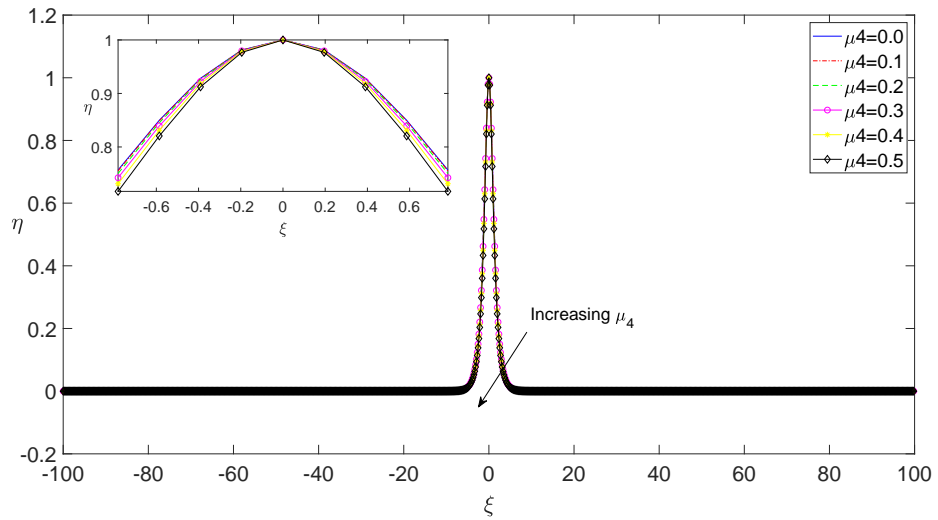


Figure 5.16: Self-localized single soliton solution as a function of $\xi$ for various $\mu_4$ values.

peak value is conserved for increasing values of $\mu_4 = 0.0, 0.1, 0.2, 0.3, 0.4, 0.5$.

In Fig. (5.17), we show the self-localized single soliton power as a function of soliton eigenvalue, $\mu$. It is known that one of the necessary conditions is the slope
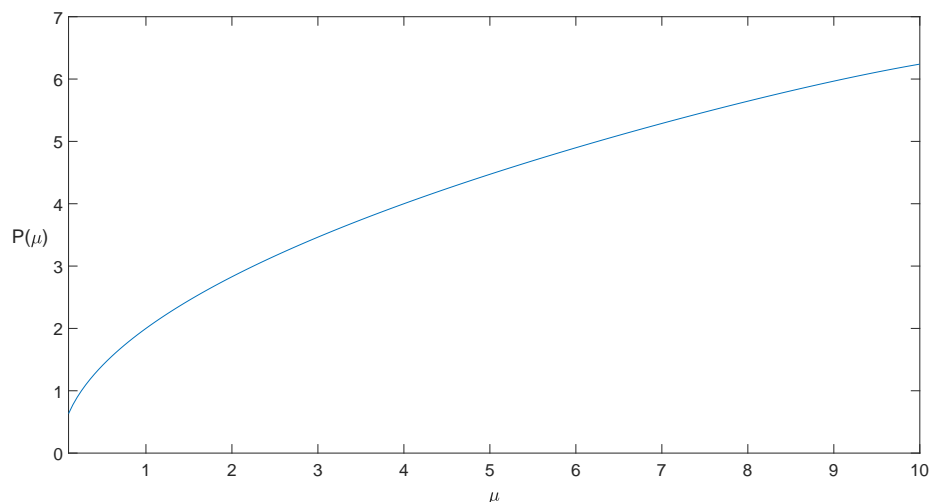
Figure 5.17: Self-localized single soliton solution power as a function of soliton eigenvalue, $\mu$.

condition $dP/d\mu \geq 0$ for the soliton stability where

$$P = \int_{-L}^{+L} |U|^2 \, dx \tag{5.2}$$

is the soliton power. This condition is also known as Vakhitov-Kolokolov condition [79–81]. We depict the soliton power as a function of soliton eigenvalue in Fig. (5.17) for the values of $\mu \in [0, 100]$. Clearly, it can be observed that Vakhitov-Kolokolov slope condition is satisfied.

The second condition, for the slope stability is the spectral condition [79–81]. One can perform an eigenvalue analysis of the operator of the governing equation for this purpose. Alternatively, checking the stability of such solitons via a numerical scheme is a more popular choice. For this purpose, we use the SSFM and perform the time stepping of the self-localized single soliton of the KEE as an initial condition in the SSFM. We plot the soliton power as a function of time obtained using SSFM in Fig. (5.18). As Fig. (5.18) confirms, the soliton power remains bounded during time stepping with a small amount of distortion due to round-off errors of the SSFM. This result suggests the stability of the self-localized single soliton of the KEE, which is no surprise since the analytical forms of this

29
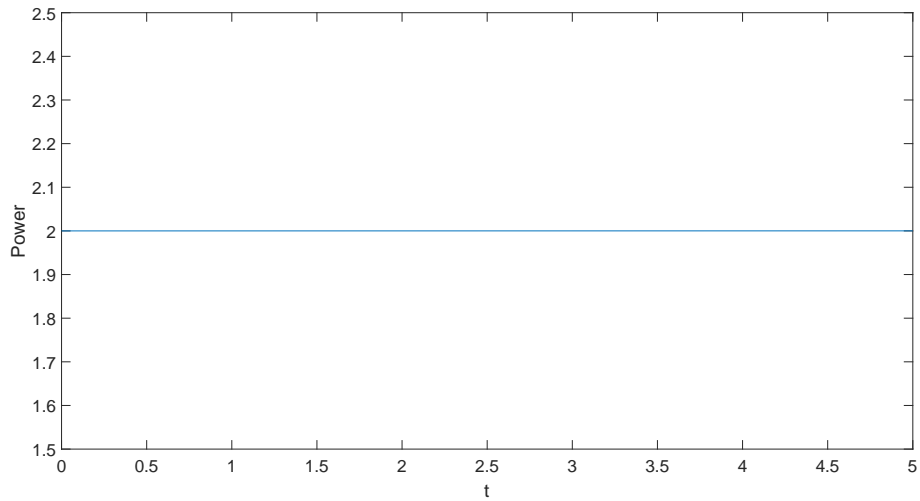
Figure 5.18: Self-localized single soliton solution power as a function of time under no dissipation, $\mu_3 = 0$.
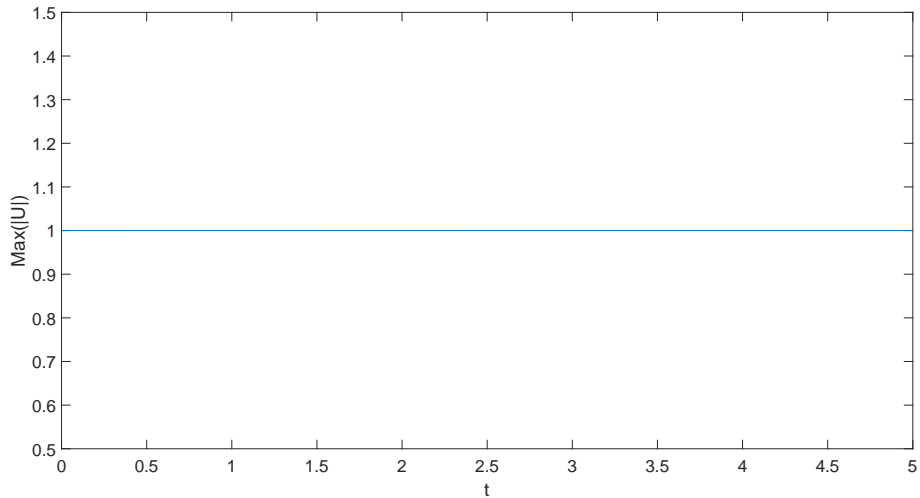


Figure 5.19: Self-localized single soliton peak amplitude as a function of time under no dissipation, $\mu_3 = 0$.

solution are given in [33,58]. In order to investigate the self-localized single soliton dynamics during time stepping, we depict Fig. (5.20).

In Fig. (5.20), the real part, imaginary part and absolute value of U is depicted for two different times of $t = 0$ and $t = 5$. As this figure confirms, the validity of the numerical solution is achieved since a stable behavior of the soliton is observed
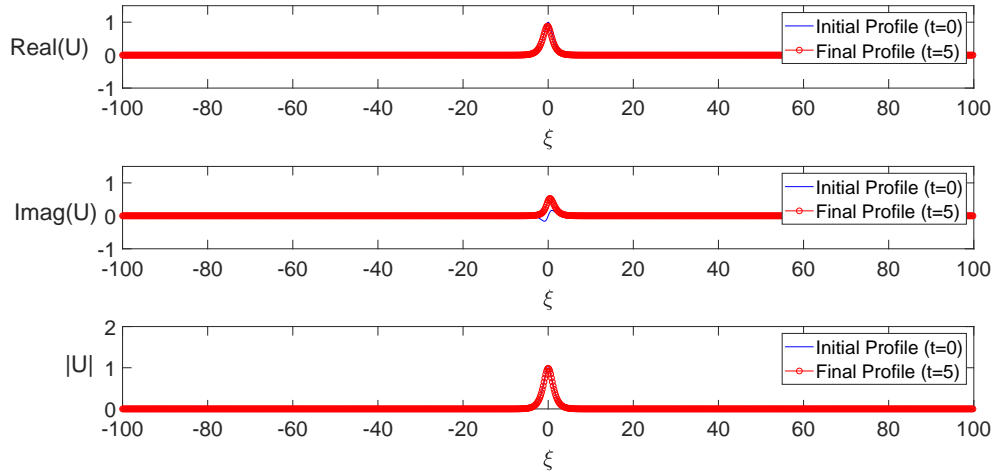
Figure 5.20: Self-localized single soliton solution at two different times $t = 0$ and $t = 5$ for $\mu_3 = 0$; a) Real part of U, b) Imaginary part of U, c) Absolute value of U.

and its peak is conserved at these two different times.
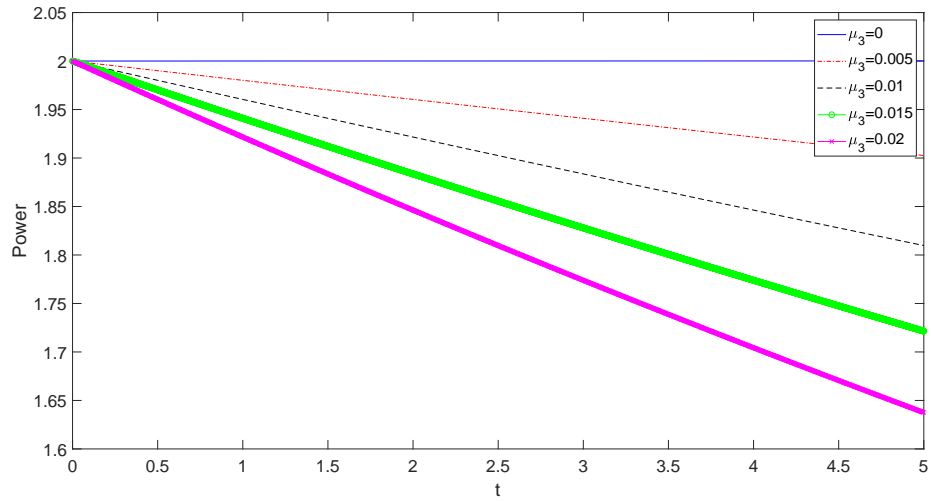


Figure 5.21: Self-localized single soliton power as a function of time for various dissipation parameter, $\mu_3$, values.

If such a self-localized single soliton of the KEE undergoes a dissipative process, it is likely that the soliton power and its properties will change. In order to investigate the effects of dissipation parameter on soliton power and the peak soliton amplitude, we depict Fig. (5.21) and Fig. (5.22) for various values of $\mu_3$.
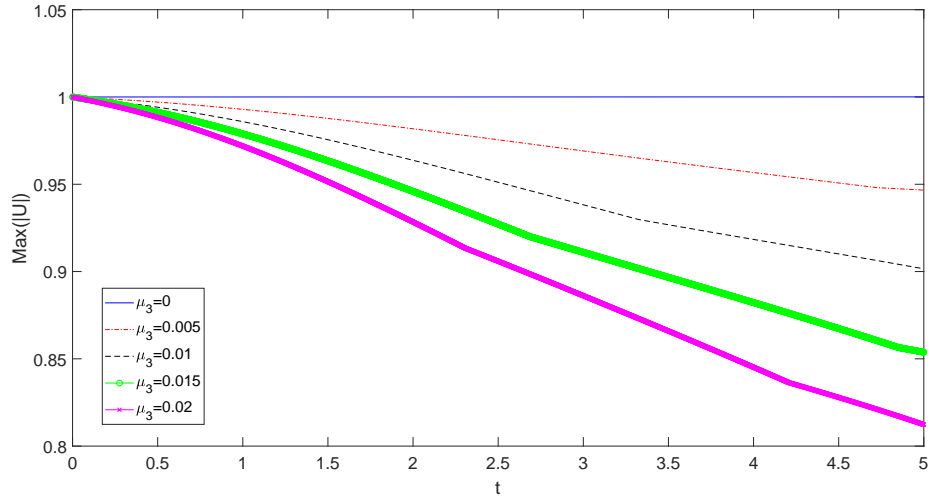
Figure 5.22: Self-localized single soliton peak amplitude as a function of time for various dissipation parameter, $\mu_3$, values.

While such a dissipation term will dissipate out the stable self-localized single soliton of the KEE, it will render as an important parameter for the soliton stabilization when the photorefractive potential term will show up in the coming sections of this thesis.

### 5.3.2 Two soliton

In this section, we perform the similar analysis for self-localized two soliton solution of the KEE. With this aim, we start PM numerical solutions with an initial condition which has two Gaussians superimposed. The convergence criteria of the PM simulations is relaxed to normalized change of $\alpha$ to be less than $1 \times 10^{-5}$. In these numerical simulations, we observe that the initial condition rapidly converges to the self-localized to soliton solution of the KEE. As before we depict the self-localized two soliton shapes in Fig. (5.23), Fig. (5.24) and Fig. (5.25) for various values of $\mu_1$, $\mu_2$ and $\mu_4$, respectively. The characteristics and changes of the soliton shapes with changing coefficients is similar to the one soliton case discussed above.
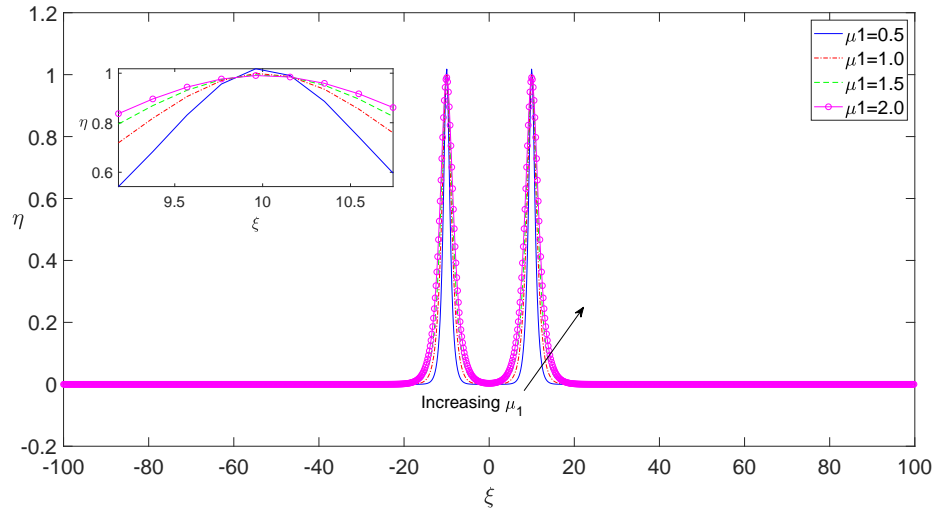
Figure 5.23: Self-localized two soliton solution as a function of $\xi$ for various $\mu_1$ values.
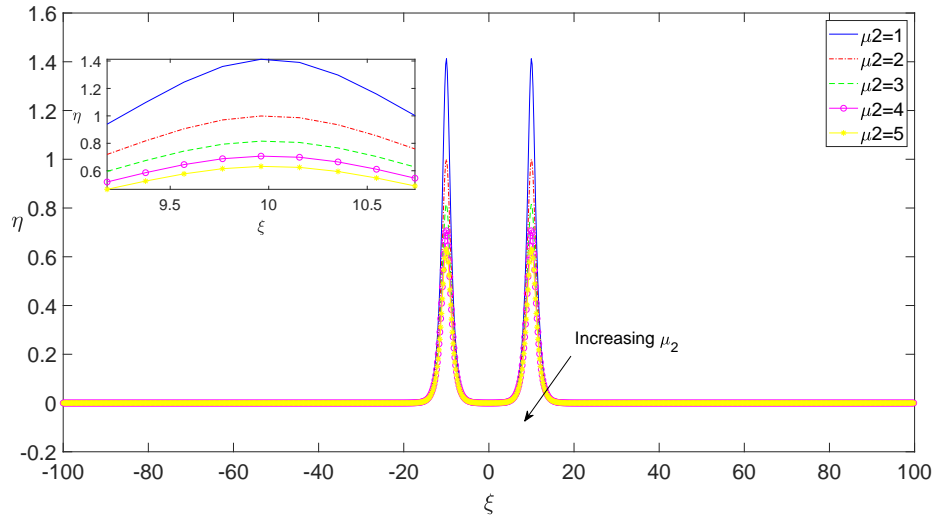


Figure 5.24: Self-localized two soliton solution as a function of $\xi$ for various $\mu_2$ values.

Similar to the one soliton case, we depict the two soliton power as a function of soliton eigenvalue, $\mu$, in Fig. (5.26). The behavior of power presented in this figure also confirms that the Vakhitov-Kolokolov slope condition is satisfied for the self-localized two soliton solution of the KEE. As before, this result is not surprising and is in accordance with the analytical results given in [33, 58].

Figure 5.25: Self-localized two soliton solution as a function of $\xi$ for various $\mu_4$ values.
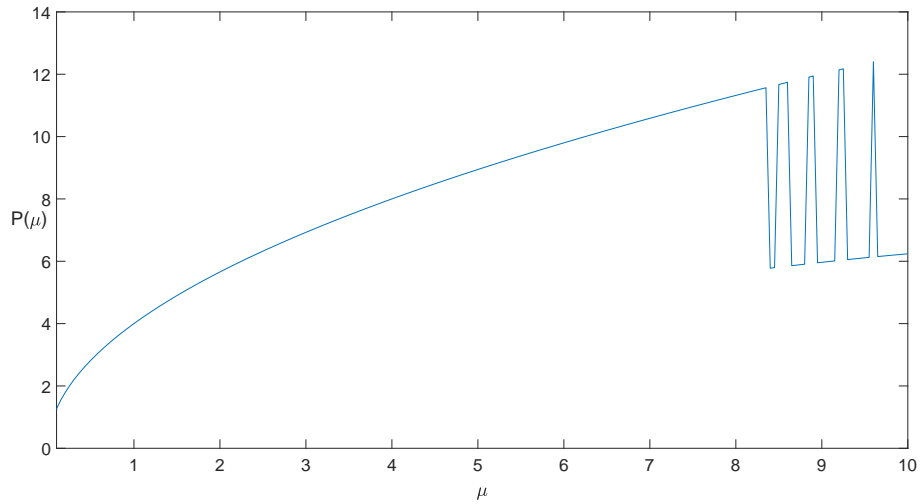


Figure 5.26: Self-localized two soliton solution power as a function of soliton eigenvalue, $\mu$.

However, as mentioned before the Vakhitov-Kolokolov slope condition is a necessary but not sufficient condition. Therefore, it is mandatory to check the temporal dynamics of the two soliton solution. As before, taking this two soliton solution as our initial condition, we perform time integration via SSFM described before. As indicated in Fig. (5.27) and Fig. (5.28), the self-localized two soliton power and the peak soliton amplitude remains almost constant when small round-off

errors are ignored. This finding suggests the stability of the soliton, as expected.
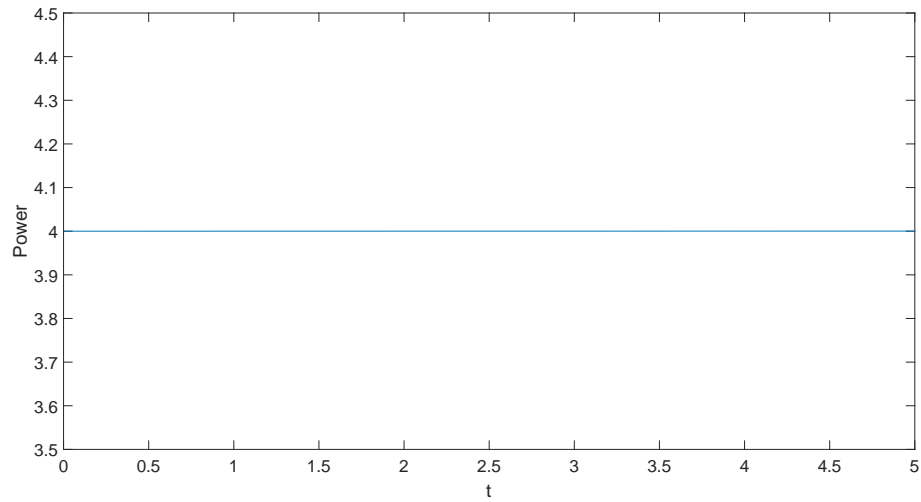


Figure 5.27: Self-localized two soliton solution power as a function of time under no dissipation, $\mu_3 = 0$.
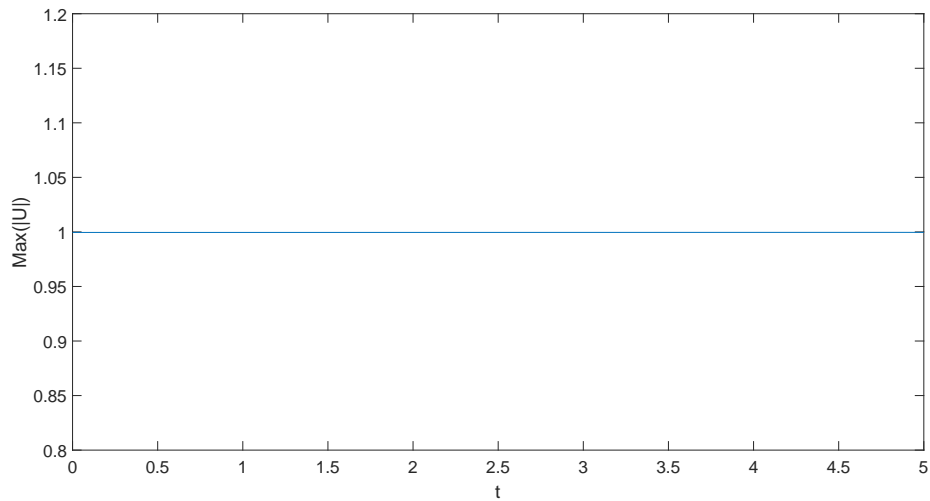


Figure 5.28: Self-localized two soliton peak amplitude as a function of time under no dissipation, $\mu_3 = 0$.

Checking Fig. (5.29), where the two soliton solution is depicted at two different times of $t = 0$ and $t = 5$, we observe that two peaks of the soliton are conserved which confirms both the stability of the soliton and the accuracy of SSFM, considering the exact analytical solutions.

Figure 5.29: Self-localized two soliton solution at two different times $t = 0$ and $t = 5$ for $\mu_3 = 0$; a) Real part of U, b) Imaginary part of U, c) Absolute value of U.



Figure 5.30: Self-localized two soliton power as a function of time for various dissipation parameter, $\mu_3$, values.

Lastly, we check the effect of dissipation parameter on the power and the peak amplitude of the two soliton solution and depict our findings in Fig. (5.30) and Fig. (5.31). In this figure, various values of $\mu_3$ is considered and it is observed that even a small value of this parameter has a strong effect to dissipate the two soliton solution. The analysis presented here will be more critical when the stabilization of such solitons under the effect of photorefractive potential considered in the

Figure 5.31: Self-localized two soliton peak amplitude as a function of time for various dissipation parameter, $\mu_3$, values.

next sections of this work.

### 5.3.3 Three soliton

We extend the analysis presented above for the single and two soliton solutions of the KEE to its three soliton solution. In order to reconstruct the three soliton solutions we begin PM simulations using an initial condition where we superimposed three Gaussians. In our simulations, we observe that it is customary to relax the convergence criteria to normalized change of $\alpha$ to be less than $1 \times 10^{-2}$. Otherwise, we observed that three Gaussians may converge to self-localized single or two soliton solutions.

Following the analysis performed for the single and two solitons of the KEE, we present the self-localized three soliton solutions of the KEE in Fig. (5.32), Fig. (5.33) and Fig. (5.34) for various values of $\mu_1$, $\mu_2$ and $\mu_4$, respectively, and we observe a similar tendency in the soliton properties for changing values of these parameters.
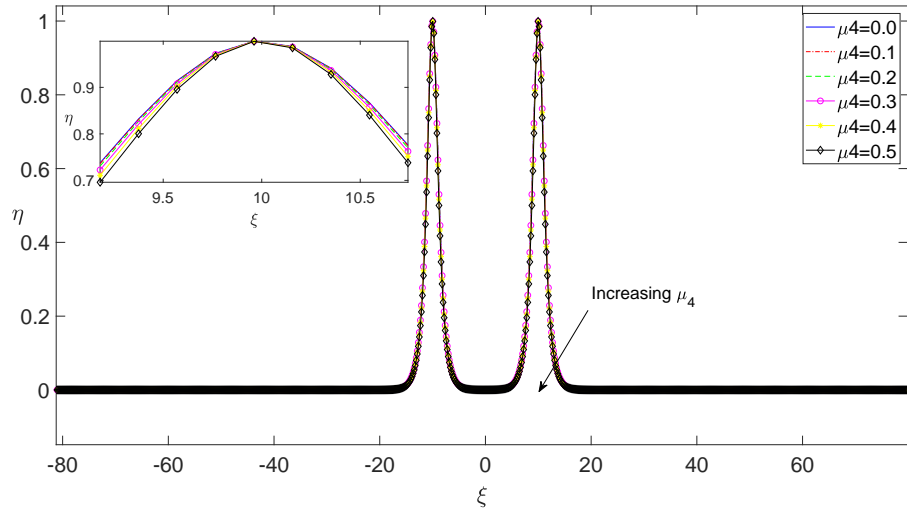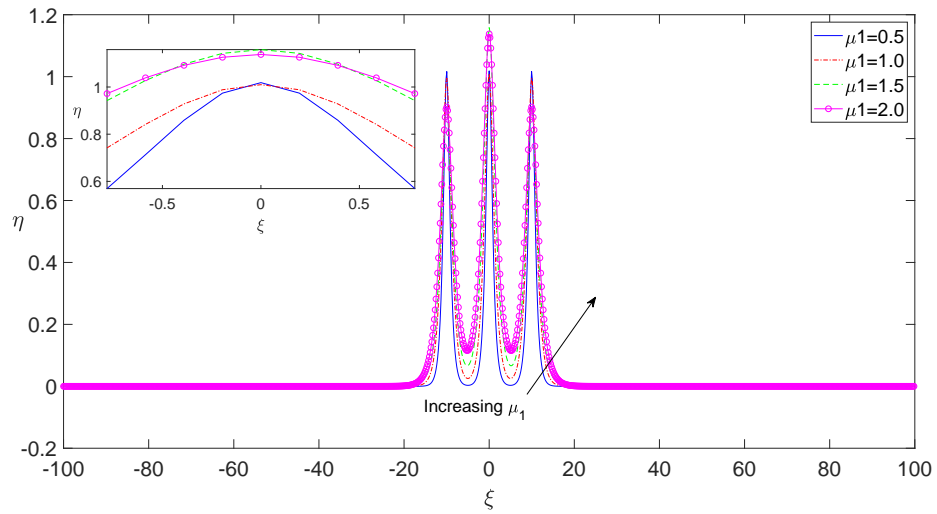
Figure 5.32: Self-localized three soliton solution as a function of $\xi$ for various $\mu_1$ values.
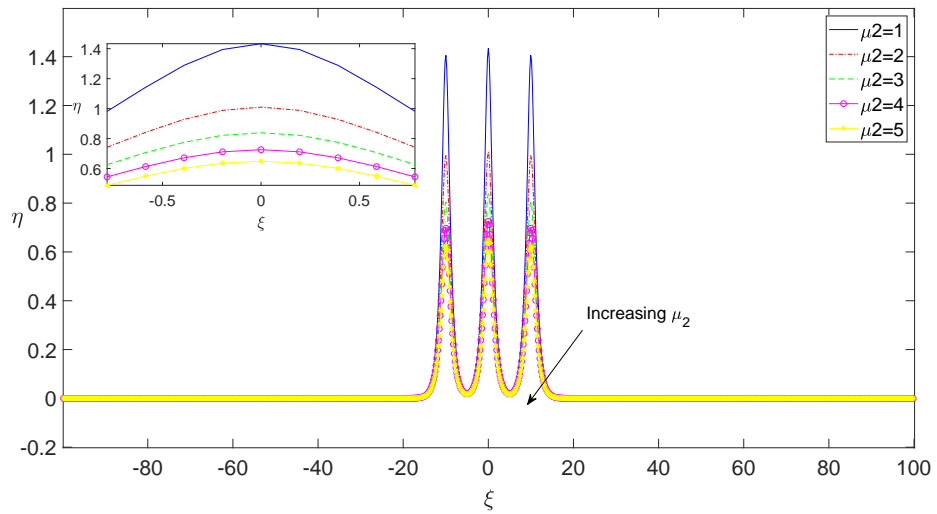


Figure 5.33: Self-localized three soliton solution as a function of $\xi$ for various $\mu_2$ values.

In order to analyze the stability and temporal dynamics of the self-localized three soliton solution we depict Fig. (5.35), Fig. (5.36), Fig. (5.37) and Fig. (5.38), in which we present soliton eigenvalue-power graph, time-power graph, time-peak soliton amplitude graph and the three soliton solution at two different times. As these figures confirm, our numerical simulations indicate that three soliton solution of the KEE turns out to be stable in accordance with the analytical solutions. Similarly, the time-power graph given in Fig. (5.39) calculated using
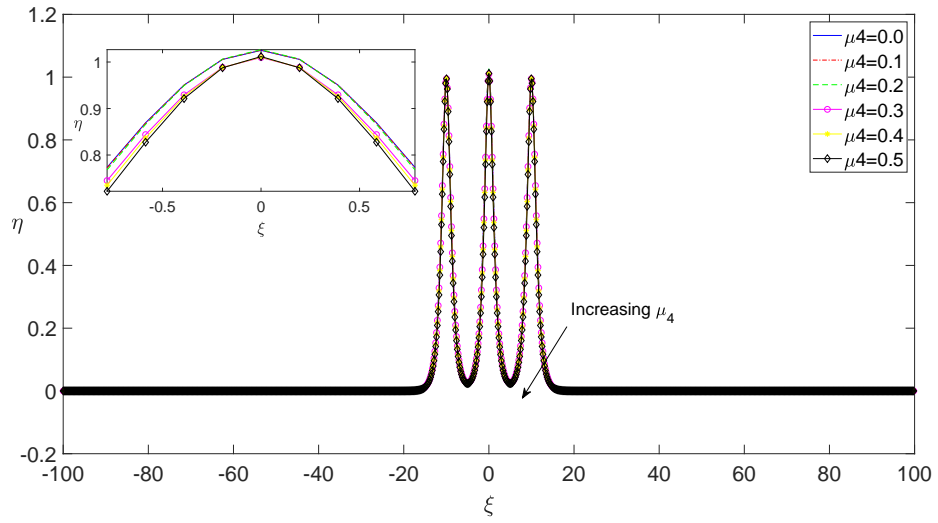
Figure 5.34: Self-localized three soliton solution as a function of $\xi$ for various $\mu_4$ values.
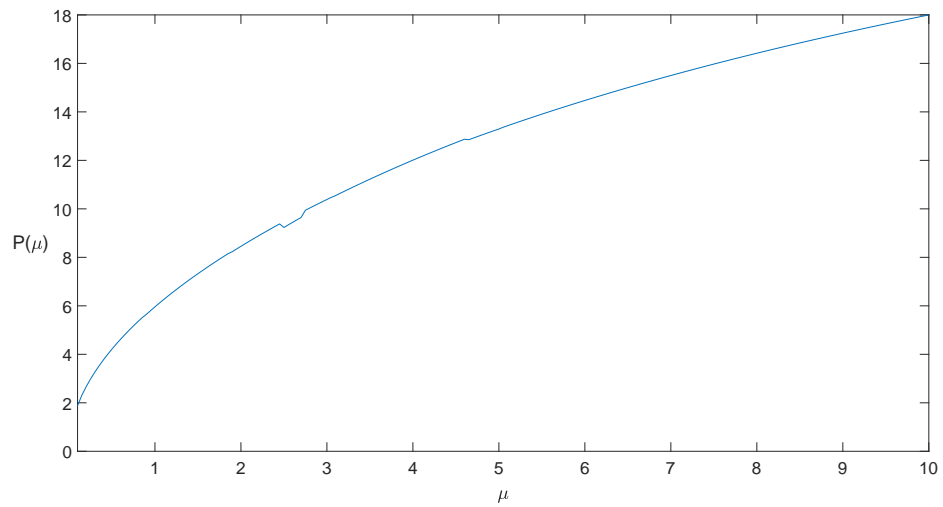


Figure 5.35: Self-localized three soliton solution power as a function of soliton eigenvalue, $\mu$.

various values of $\mu_3$ shows that a small dissipation parameter can have significant effect on the soliton stability and dissipate it within short time scales.
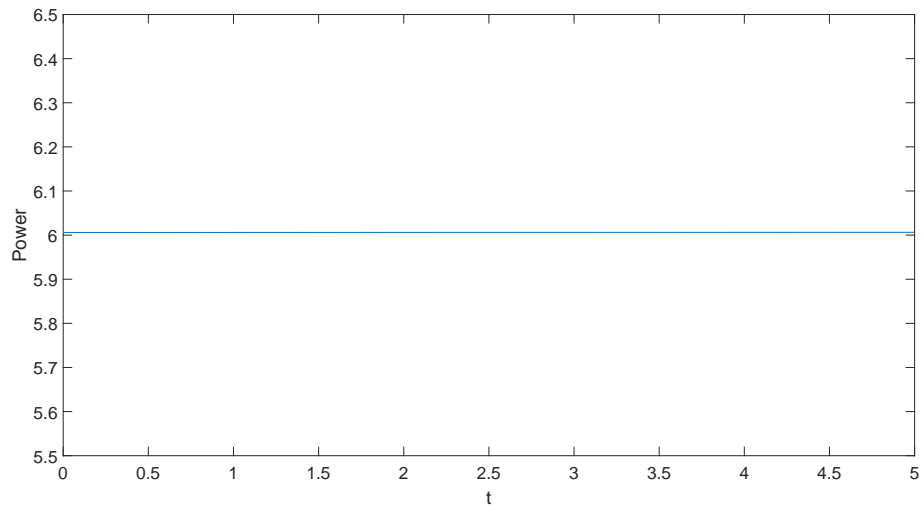
Figure 5.36: Self-localized three soliton solution power as a function of time under no dissipation, $\mu_3 = 0$.
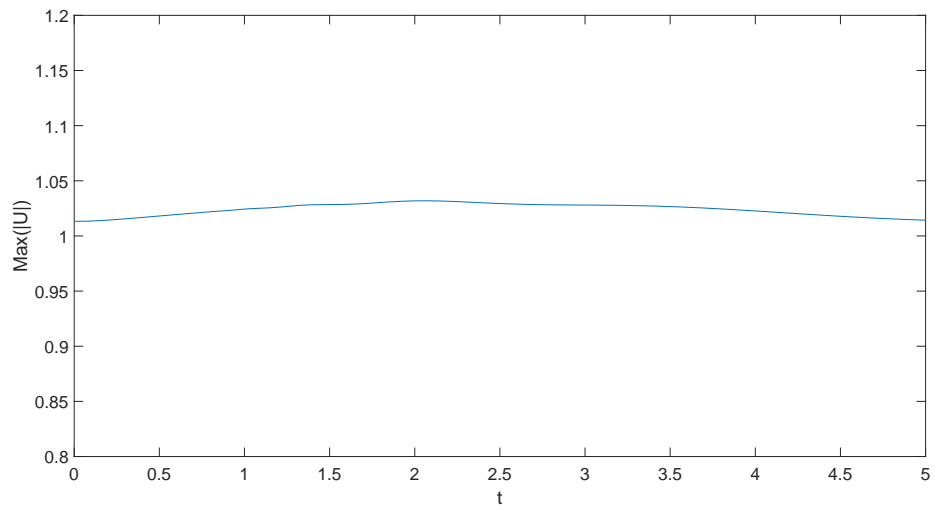


Figure 5.37: Self-localized three soliton peak amplitude as a function of time under no dissipation, $\mu_3 = 0$.
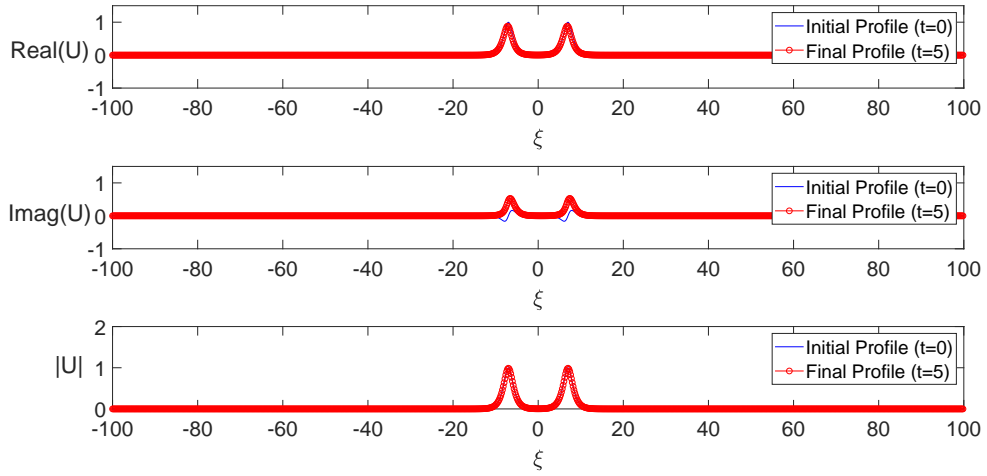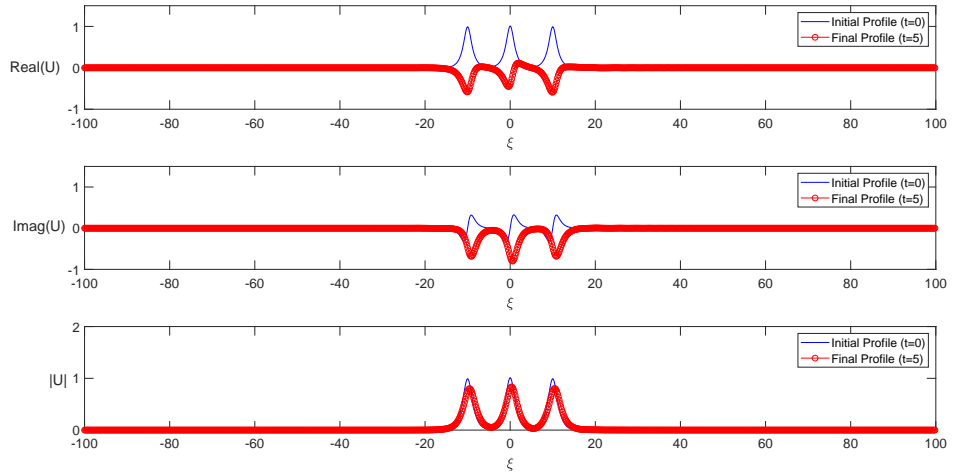
Figure 5.38: Self-localized three soliton solution at two different times $t = 0$ and $t = 5$ for $\mu_3 = 0$; a) Real part of U, b) Imaginary part of U, c) Absolute value of U.
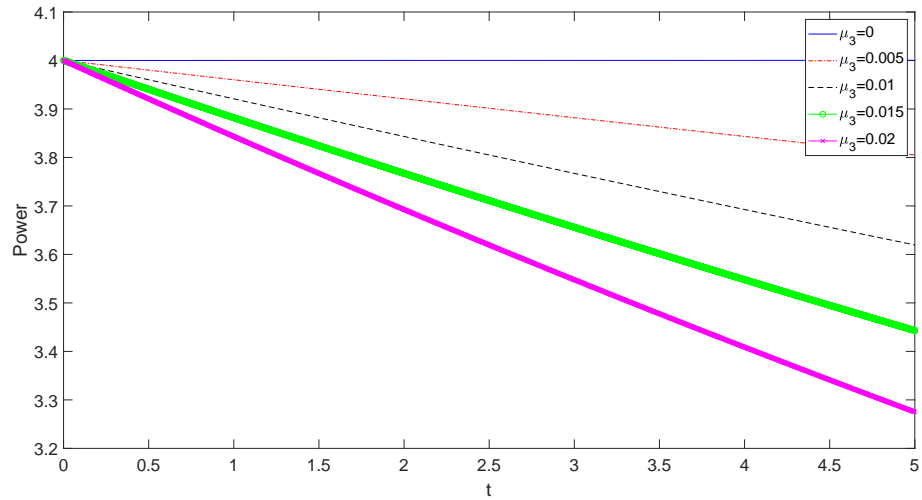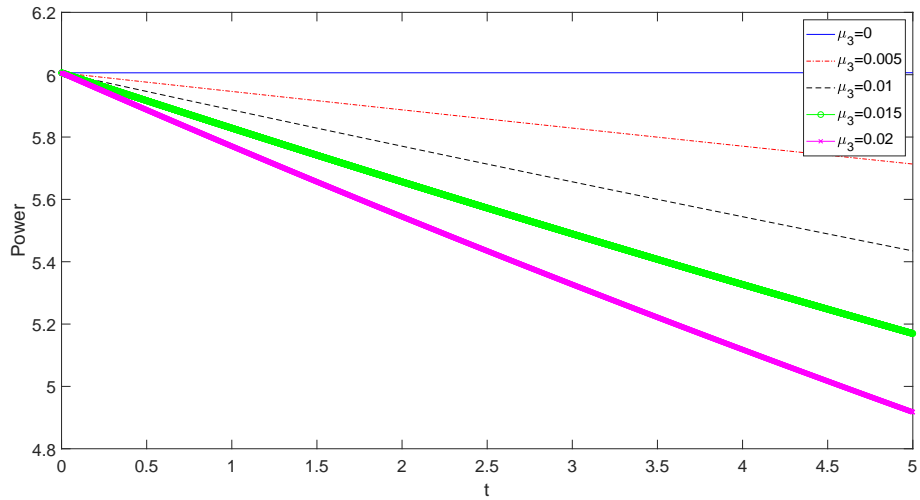


Figure 5.39: Self-localized three soliton solution power as a function of time for various dissipation parameter, $\mu_3$, values.

## 5.4 Results and Discussion of the Self-Localized Solutions of the Dissipative Kundu-Eckhaus Equation with Photorefractive Potential Obtained by Petviashvili Method

In this section, we extend the analysis presented in the preceding section to include the effects of a potential term. More specifically, we consider the dynamics of self-localized single, two and three soliton solutions of the KEE under the effect of

41
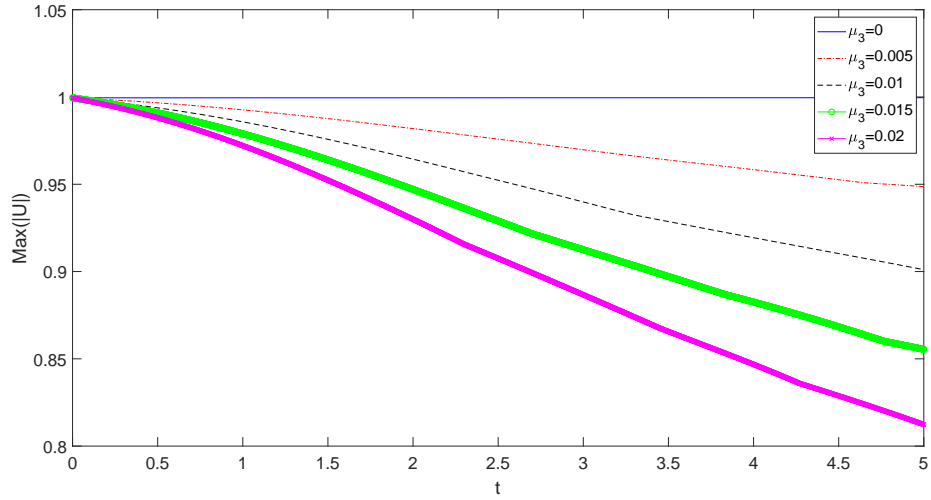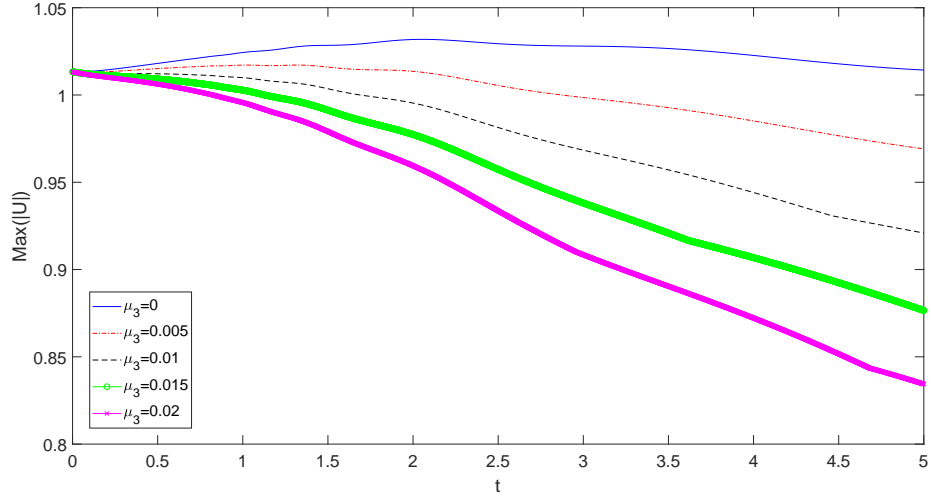
Figure 5.40: Self-localized three soliton peak amplitude as a function of time for various dissipation parameter, $\mu_3$, values.

the photorefractive potential term given as $V(\xi) = I_o \cos^2(\xi)$, where $I_0 = 2.5$ as before. To our best knowledge, the analytical solutions of such a system is unknown. With this motivation, we perform the numerical solutions of the KEE with the photorefractive potential term using Eq.(4.14) and Eq.(4.15). A recent analysis on KEE having photorefractive and saturable type of nonlinearities show that its self-localized single, two and three soliton solutions are unstable [78]. In here, we show that those solitons can be stabilized using a dissipation parameter which physically models a dissipative medium. With this motivation, we perform the time integration of these solitons using SSFM considering the effects of dissipation and show that self-localized single, two and three soliton solutions can be stabilized in a dissipative medium.

### 5.4.1 Single soliton

As before, using the same computational parameters utilized for the numerical simulations in the preceding part and using a convergence criteria as the normalized change of $\alpha$ to be less than $1 \times 10^{-10}$, we construct the self-localized single soliton solution of the KEE under the effect of dissipation. In here, the initial

condition is taken to be a Gaussian as before. In Fig. (5.41), Fig. (5.42) and Fig. (5.43), we depict the self-localized single soliton of the KEE under the effect of the photorefractive potential term for various values of $\mu_1$, $\mu_2$ and $\mu_4$. The similar changes soliton profile changes observed for the KEE having no potential can be observed for the changing values of $\mu_1$, $\mu_2$ and $\mu_4$.
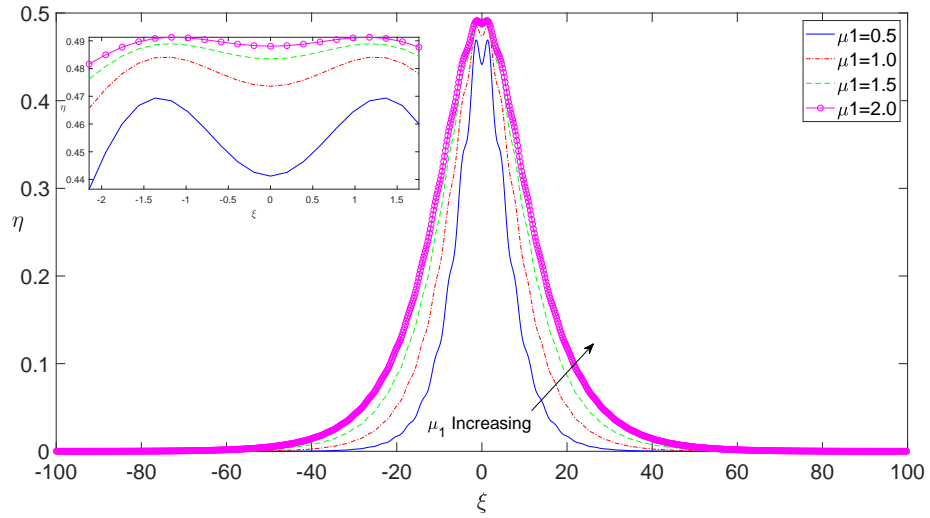


Figure 5.41: Self-localized single soliton solution as a function of $\xi$ for various $\mu_1$ values with photorefractive potential.
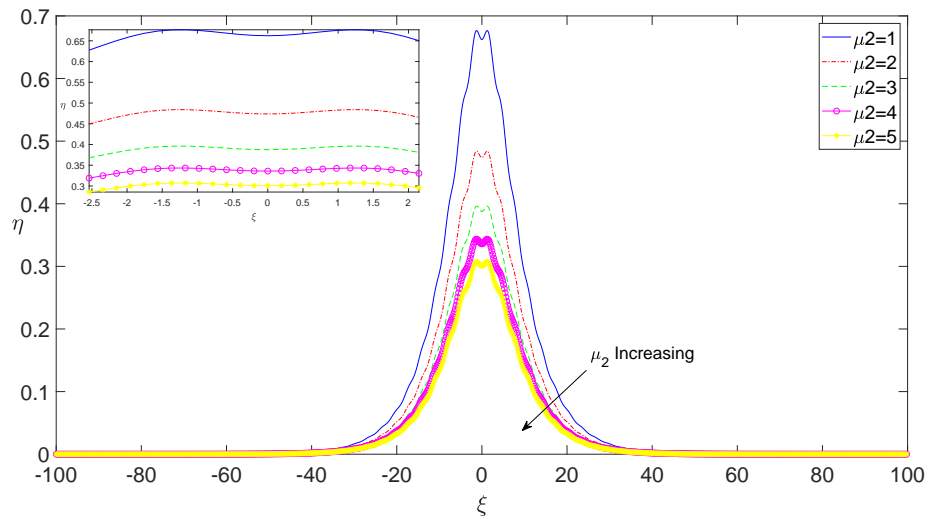


Figure 5.42: Self-localized single soliton solution as a function of $\xi$ for various $\mu_2$ values with photorefractive potential.
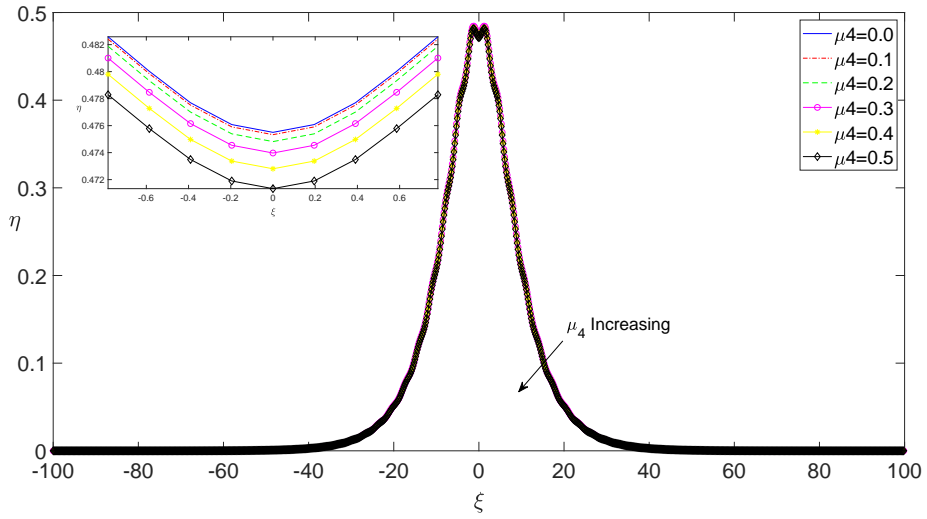
Figure 5.43: Self-localized single soliton solution as a function of $\xi$ for various $\mu_4$ values with photorefractive potential.

As Fig. (5.41), Fig. (5.42) and Fig. (5.43) confirm, the self-localized single soliton solution of the KEE under the effect of a photorefractive potential term can be constructed using the PM. The significant effect of potential on this soliton is a dip on its peak, similar to the effects discussed in [74] for the NLSE. However, a recent analysis showed that it is unstable for the soliton eigenvalues, $\mu$, considered [78]. Such an unstable behavior can also be observed for our simulations as depicted in Fig. (5.44), Fig. (5.45) and Fig. (5.46), that is although Vakhitov-Kolokolov condition is satisfied, the solutions grow unboundedly in time.

In order to discuss the stability and observe the temporal dynamics of the self-localized single soliton solution of the KEE with the photorefractive potential, we again perform its time integration using the SSFM. The time-power and time-peak amplitude graphs obtained for this soliton are depicted in Fig. (5.45) and Fig. (5.46), which clearly exhibits an unstable behavior for the non-dissipative case.

In this thesis, we argue the uses of dissipation to stabilize such solitons. Starting from the self-localized single soliton solution of the KEE with photorefractive potential term, we perform its numerical time integration using the dKEE model
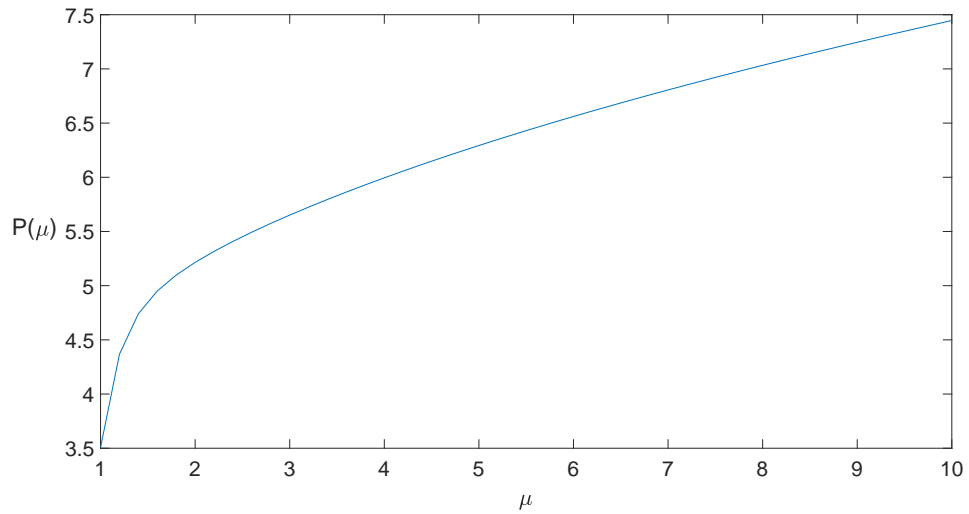
Figure 5.44: Self-localized single soliton solution power as a function of soliton eigenvalue, $\mu$, with photorefractive potential.
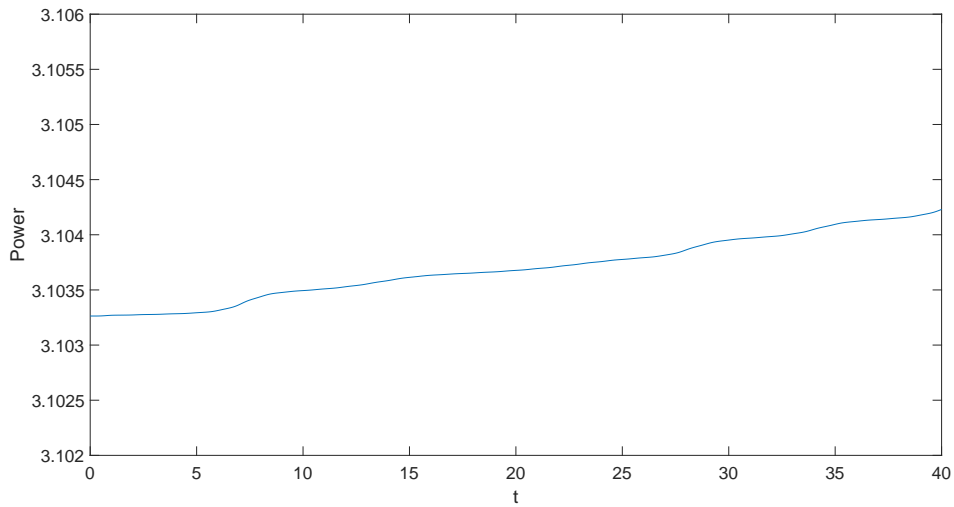


Figure 5.45: Self-localized single soliton solution power as a function of time under no dissipation, $\mu_3 = 0$ with photorefractive potential.

for various values of the dissipation parameter and depict the time-power graph for these values in Fig. (5.47).

By checking Fig. (5.47) and Fig. (5.48), it is possible to argue that a dissipation constant of $\mu_3 = 0.01$ is enough to prevent the divergence of the power as well as the peak amplitude of the soliton. While the same behavior can be attained

Figure 5.46: Self-localized single soliton peak amplitude as a function of time under no dissipation, $\mu_3 = 0$ with photorefractive potential.



Figure 5.47: Self-localized single soliton solution power as a function of time for various dissipation parameter, $\mu_3$ with photorefractive potential.

using larger $\mu_3$, the smallest possible one is desired to keep the soliton dynamics and shapes unaffected for time scales long enough for many practical purposes. In order to illustrate the effects of dissipation parameter on the self-localized single soliton behavior, we depict Fig. (5.49). This figure presents the self-localized single soliton solution of the dKEE at two different times of $t = 0$ and $t = 40$. Although some distortion effects can be observed in the soliton shape due to

Figure 5.48: Self-localized single soliton solution peak amplitude as a function of time for various dissipation parameter, $\mu_3$ with photorefractive potential.



Figure 5.49: Self-localized single soliton solution at two different times $t = 0$ and $t = 40$ for $\mu_3 = 0.01$ with photorefractive potential; a) Real part of U, b) Imaginary part of U, c) Absolute value of U.

photorefractive potential and dissipation, one can argue that the soliton profile and localized peak are mainly conserved. This suggests that stabilization of the unstable solitons of the KEE can be achieved by taking the dissipative effects into account. In different physical context, the dissipation may refer to diverse

phenomena including but are not limited to the turbulent losses in a hydrodynamic medium or dissipation of femtosecond laser pulses used in fiber optical communication.

### 5.4.2 Two soliton

We extend the analysis summarized in the preceding section for self-localized single soliton solution of the dKEE to the two soliton solutions in this section of thesis. As before, starting from two Gaussians as the initial condition and relaxing convergence criteria as the normalized change of $\alpha$ to be $1 \times 10^{-5}$, one can numerically obtain the self-localized two soliton solution of the KEE having the photorefractive potential term using PM. Such self-localized two soliton solutions are depicted in Fig. (5.50), Fig. (5.51) and Fig. (5.52) for various values of $\mu_1$, $\mu_2$ and $\mu_4$, respectively. It can be seen in these figures that, the self-localized two soliton solutions have similar characteristics with their single soliton counterparts. Additionally, the changes in coefficients $\mu_1$, $\mu_2$ and $\mu_4$, have identifiable effects similar to those discussed in the preceding section for KEE having no and having photorefractive potential term.



Figure 5.50: Self-localized two soliton solution as a function of $\xi$ for various $\mu_1$ values with photorefractive potential.

Figure 5.51: Self-localized two soliton solution as a function of $\xi$ for various $\mu_2$ values with photorefractive potential.
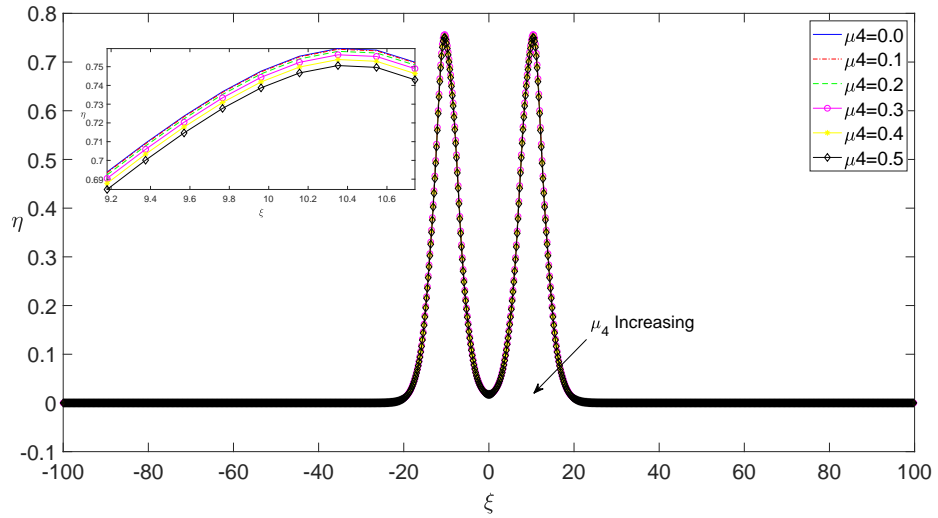


Figure 5.52: Self-localized two soliton solution as a function of $\xi$ for various $\mu_4$ values with photorefractive potential.

In order to analyze the stability characteristics of the self-localized two soliton solution of the KEE, we depict Fig. (5.53) and Fig. (5.54). Fig. (5.53) indicate that self-localized two soliton solution of the KEE satisfied the Vakhitov-Kolokolov slope condition necessary for soliton stability, however Fig. (5.54) and Fig. (5.55) show that soliton power and peak amplitude do not remain bounded during time stepping as discussed before and in [78].

Figure 5.53: Self-localized two soliton solution power as a function of soliton eigenvalue, $\mu$ with photorefractive potential.
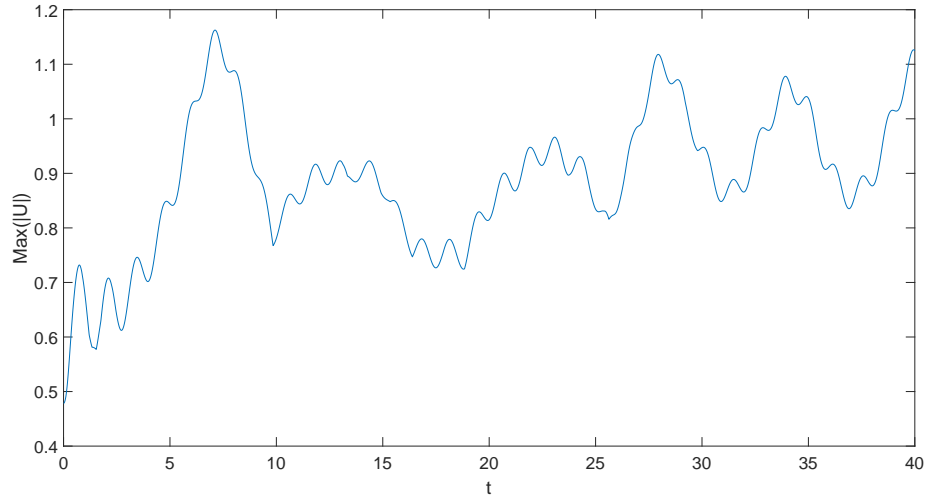


Figure 5.54: Self-localized two soliton solution power as a function of time under no dissipation, $\mu_3 = 0$ with photorefractive potential.

In order to investigate the possible stabilization of the two soliton solution by dissipation, we depict Fig. (5.56) and Fig. (5.58). As before, starting from the two soliton solution as our initial condition, we perform the time stepping of dKEE under the effect of photorefractive potential term using various values of dissipation parameter $\mu_3$. Fig. (5.56) and Fig. (5.57) confirm that the unbounded growth of the power and the peak amplitude of the two soliton solution KEE can

Figure 5.55: Self-localized two soliton peak amplitude as a function of time under no dissipation, $\mu_3 = 0$ with photorefractive potential.
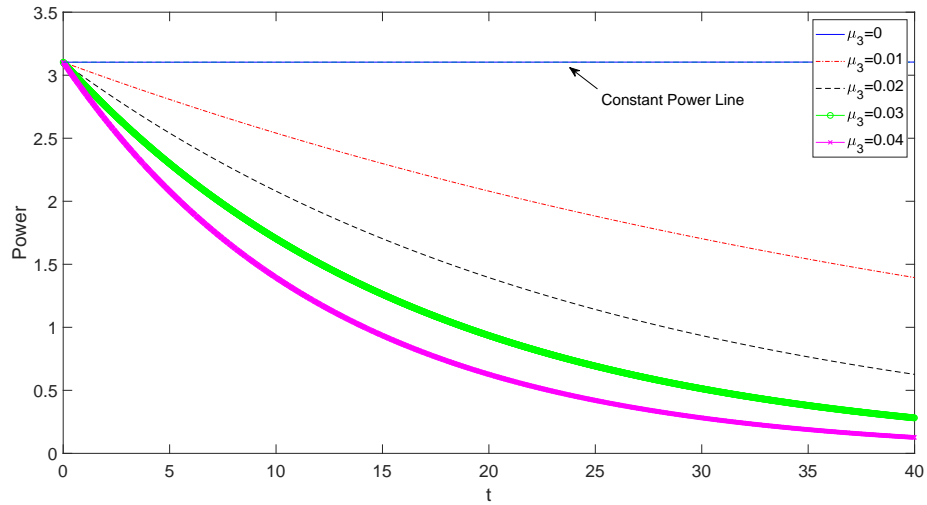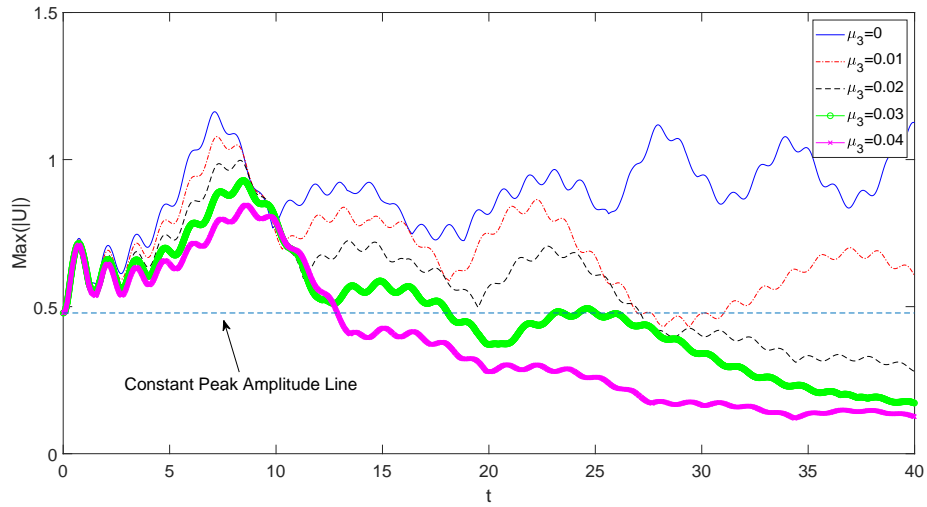


Figure 5.56: Self-localized two soliton solution power as a function of time for various dissipation parameter, $\mu_3$ with photorefractive potential.

be prevented using the dissipation coefficient of $\mu_3 = 0.002$.

Similar to the one soliton case, we depict Fig. (5.58) to investigate the temporal dynamics of the two soliton solution of the dKEE for $\mu_3 = 0.002$. One can realize that there is distortion in the two soliton profile due to photorefractive potential term and dissipative effects. However, as before, the two humps of the soliton

Figure 5.57: Self-localized two soliton peak amplitude as a function of time for various dissipation parameter, $\mu_3$ with photorefractive potential.
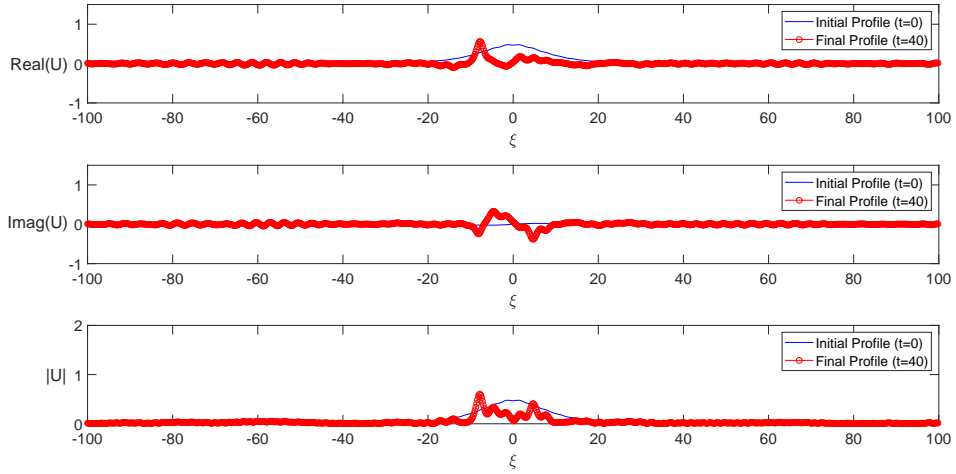


Figure 5.58: Self-localized two soliton solution at two different times $t = 0$ and $t = 40$ for $\mu_3 = 0.002$ with photorefractive potential; a) Real part of U, b) Imaginary part of U, c) Absolute value of U.

is quite well preserved even at time $t = 40$. This finding suggest the possible stabilization of the self-localized two soliton solution of the KEE using dissipative effects, while the fundamental attributes of soliton behavior is preserved.

### 5.4.3 Three soliton

Lastly, we turn our attention to the dynamics and stability characteristics of the three soliton solution of the dKEE under the effect of the photorefractive potential. With this aim, starting from an initial condition in the form of three Gaussians superimposed, we obtain the self-localized three soliton solution of the KEE using PM. As discussed for the no potential case, a relaxation of the convergence criteria defined as normalized change of $\alpha$ to be less than $1 \times 10^{-2}$ deems necessary to obtain the three solitons. As before, the effects of the various coefficients of the KEE on those soliton profile are shown in Fig. (5.59), Fig. (5.60) and Fig. (5.61).
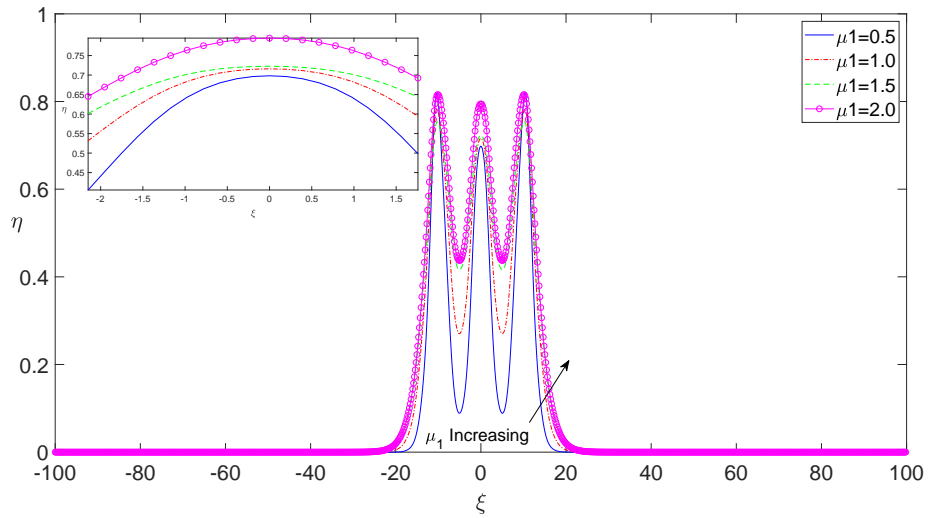


Figure 5.59: Self-localized three soliton solution as a function of $\xi$ for various $\mu_1$ values with photorefractive potential.

As these figures confirm, the three soliton solution of the KEE under the effect of photorefractive potential exhibits similar characteristics as the single and two soliton solutions. Additionally, by checking Fig. (5.62), Fig. (5.63) and Fig. (5.64), one can observe that their stability characteristics are also similar. That is, the three soliton solution satisfies the Vakhitov-Kolokolov slope condition necessary for soliton stability, however its power and peak amplitude grows unboundedly during temporal evolution.
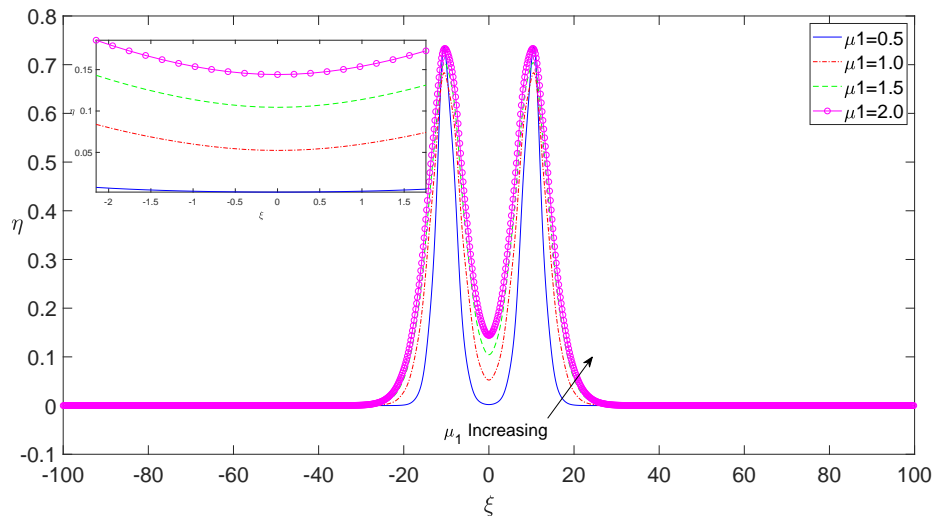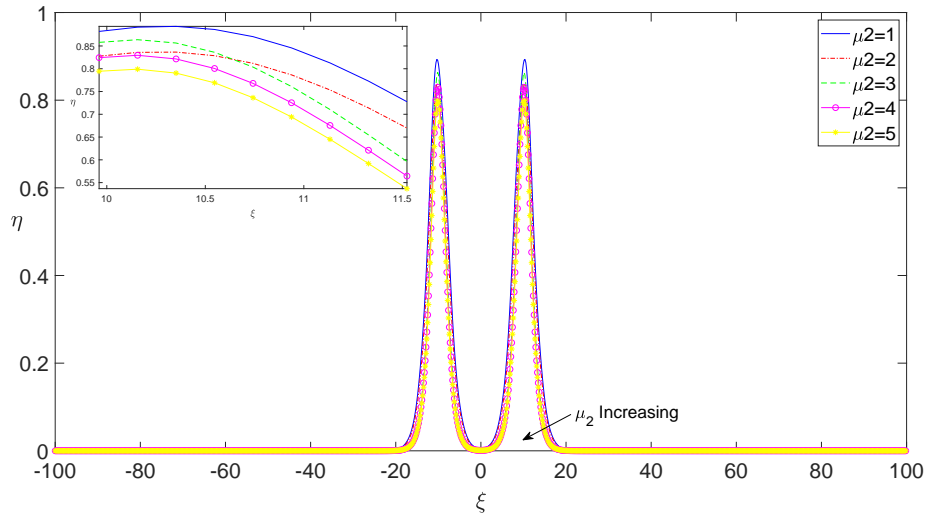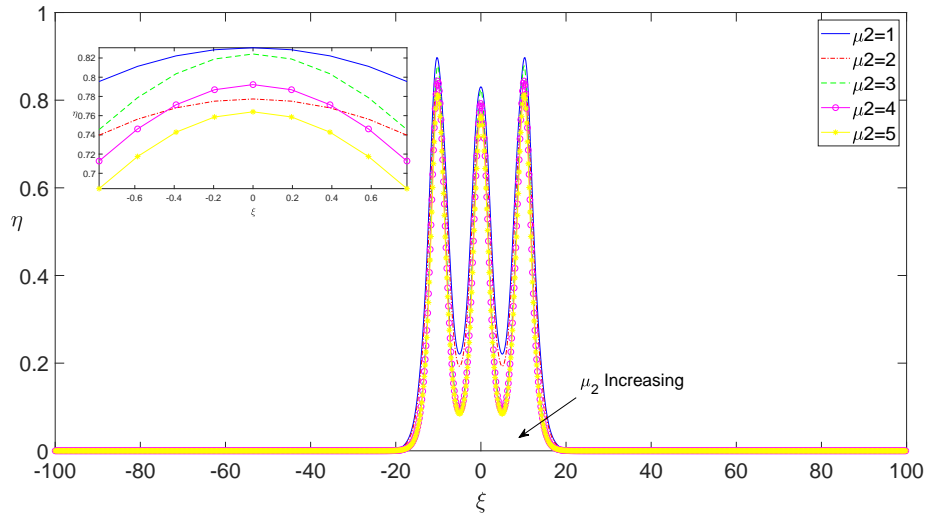
Figure 5.60: Self-localized three soliton solution as a function of $\xi$ for various $\mu_2$ values with photorefractive potential.
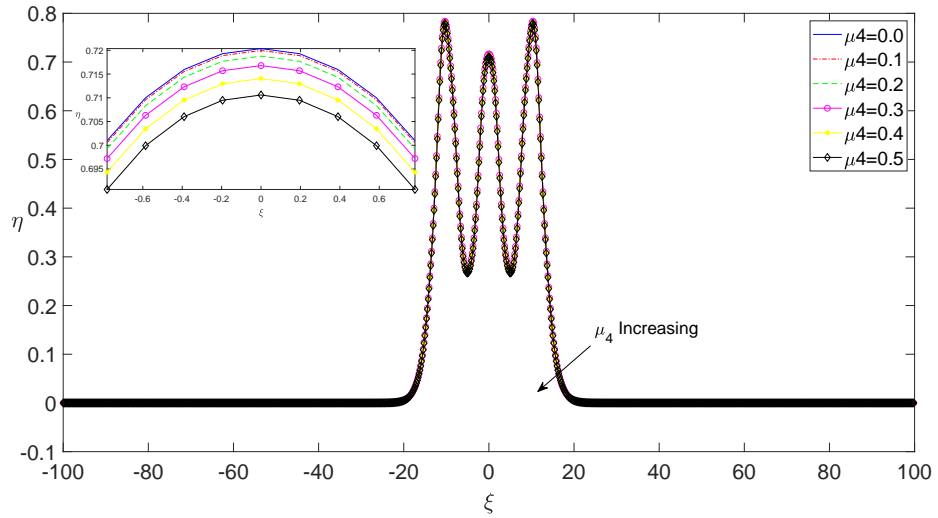


Figure 5.61: Self-localized three soliton solution as a function of $\xi$ for various $\mu_4$ values with photorefractive potential.

Similar to the previous cases, we investigate the effects of dissipation parameter on stabilization of the self-localized three soliton solution of the dKEE. For this purpose, in Fig. (5.65) we depict its time-power graph and in Fig. (5.66) we depict its time-peak amplitude graph for various values of $\mu_3$ and observe that the value of $\mu_3 = 0.002$ can be used as a minimal coefficient for its stabilization. Under the effect of this dissipation coefficient, we depict the three soliton shapes
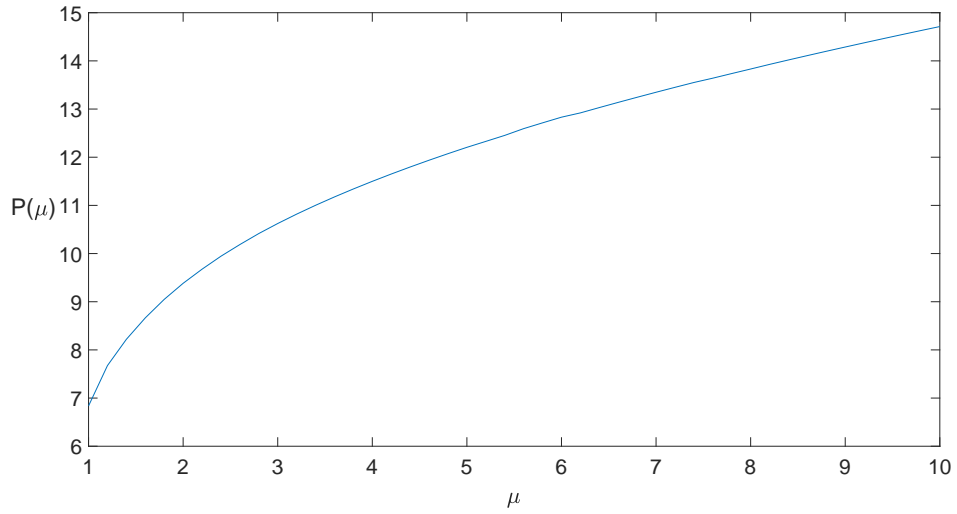
54
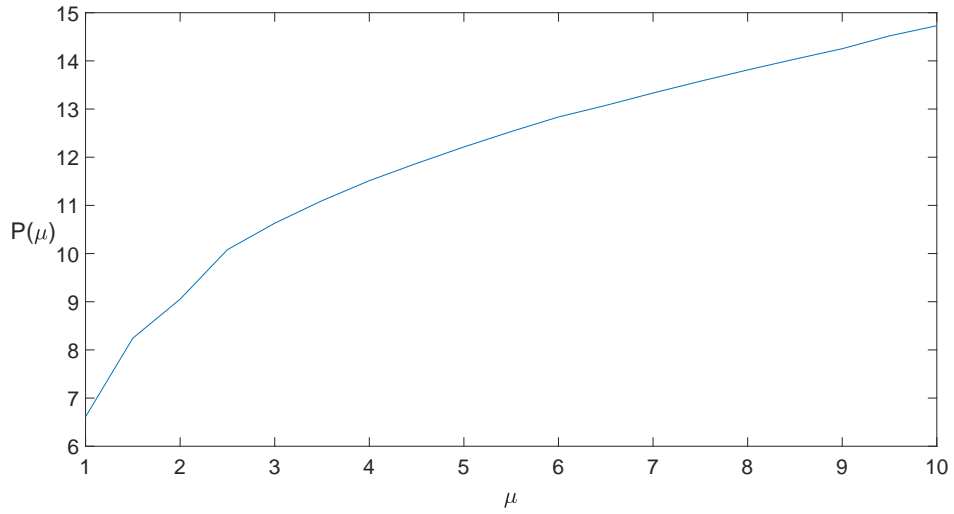
Figure 5.62: Self-localized three soliton solution power as a function of soliton eigenvalue, $\mu$ with photorefractive potential.
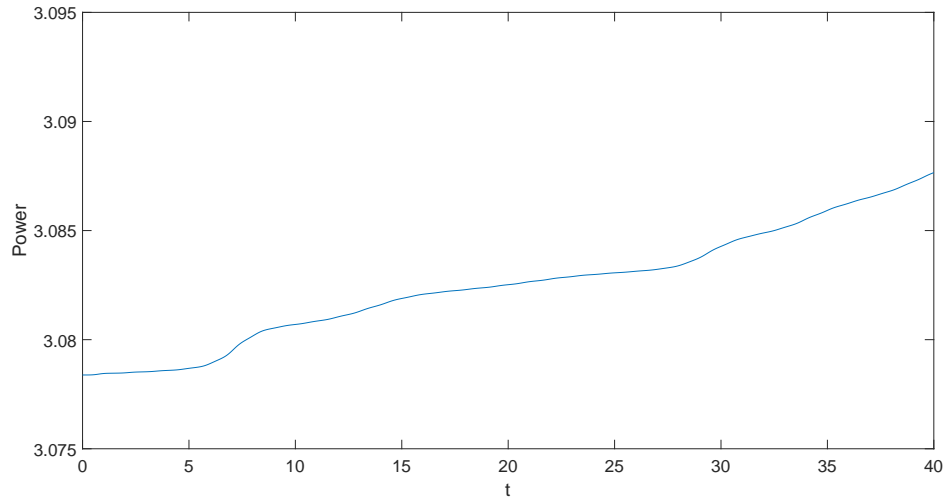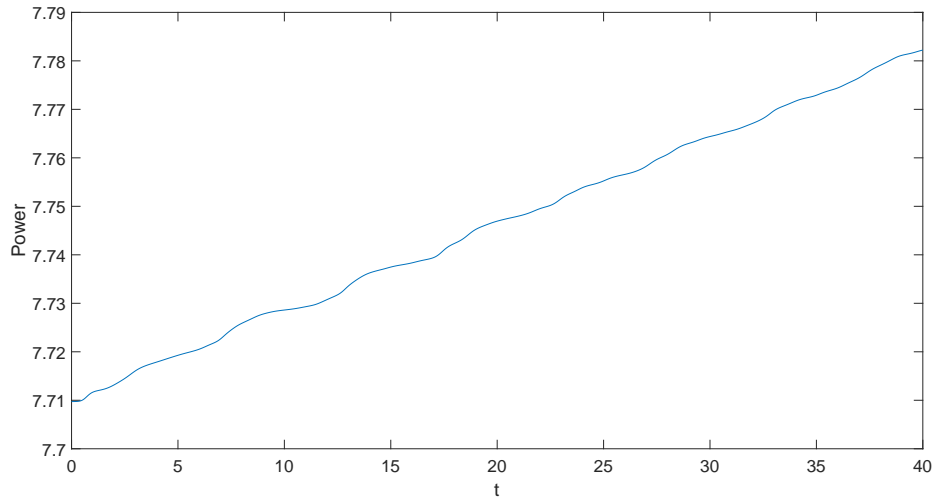


Figure 5.63: Self-localized three soliton solution power as a function of time under no dissipation, $\mu_3 = 0$ with photorefractive potential.

in Fig. (5.67) at two different times of $t = 0$ and $t = 40$. As before, the effects of photorefractive potential term and the dissipation coefficient becomes obvious in the form of distortions in the profile. However, the three soliton peaks are especially well-preserved for the absolute value of the field. This result suggests that the stabilization of the self-localized single, two, three and even N-soliton solutions of KEE is possible when dissipative effects are incorporated. Although
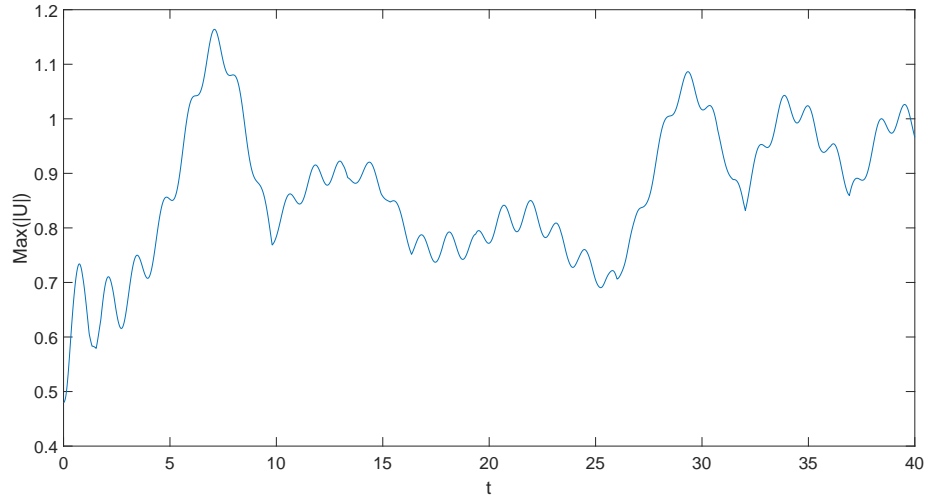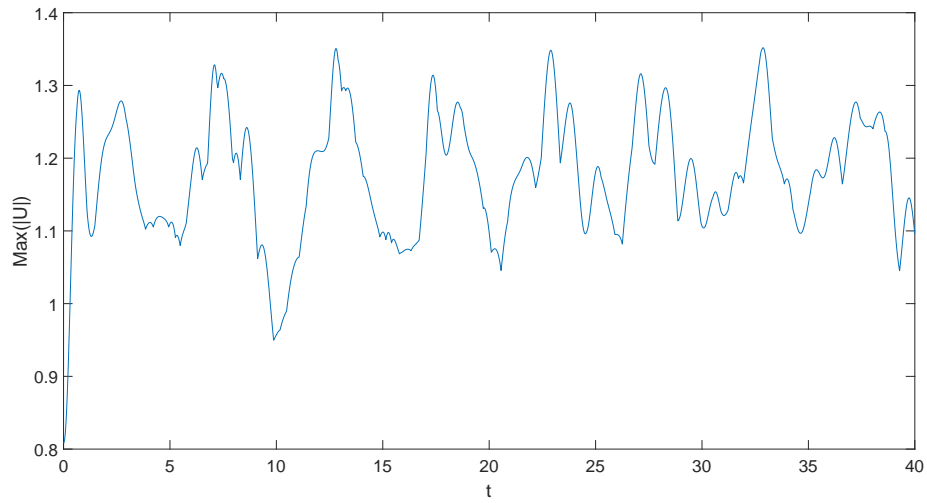
Figure 5.64: Self-localized three soliton peak amplitude as a function of time under no dissipation, $\mu_3 = 0$ with photorefractive potential.
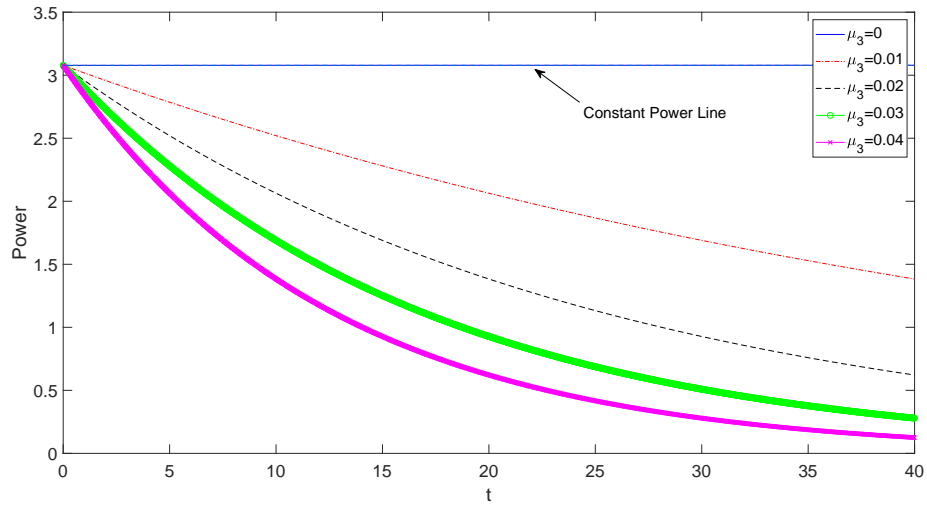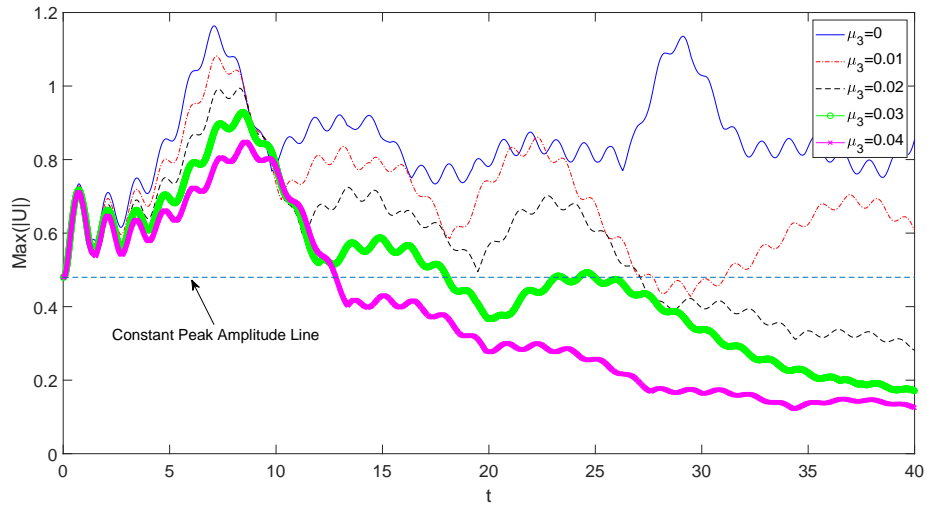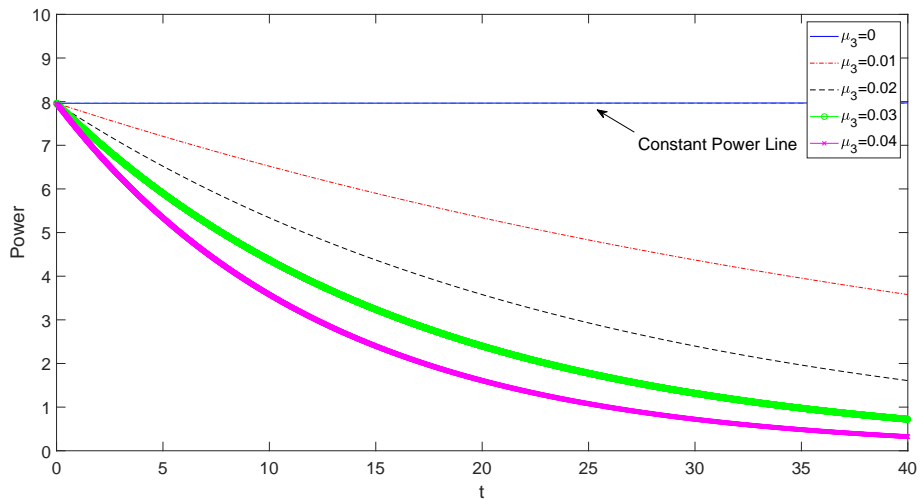


Figure 5.65: Self-localized three soliton solution power as a function of time for various dissipation parameter, $\mu_3$ with photorefractive potential.

some distortion are expected, the peak soliton shapes are relatively well-preserved for time scales considered. Depending on the phenomena modeled in the frame of KEE, various types of potential, dissipation coefficient and time scale can be used to achieve self-localized soliton stability.
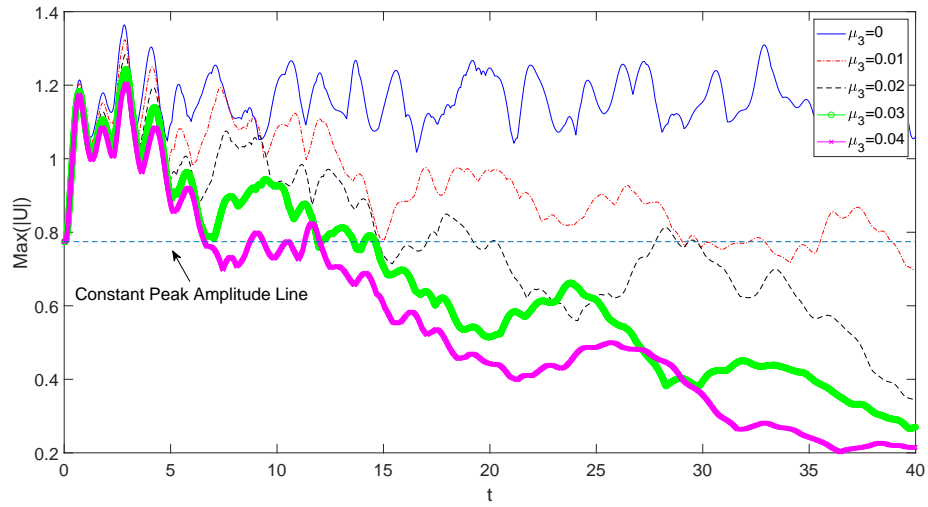
Figure 5.66: Self-localized three soliton solution peak amplitude as a function of time for various dissipation parameter, $\mu_3$ with photorefractive potential.
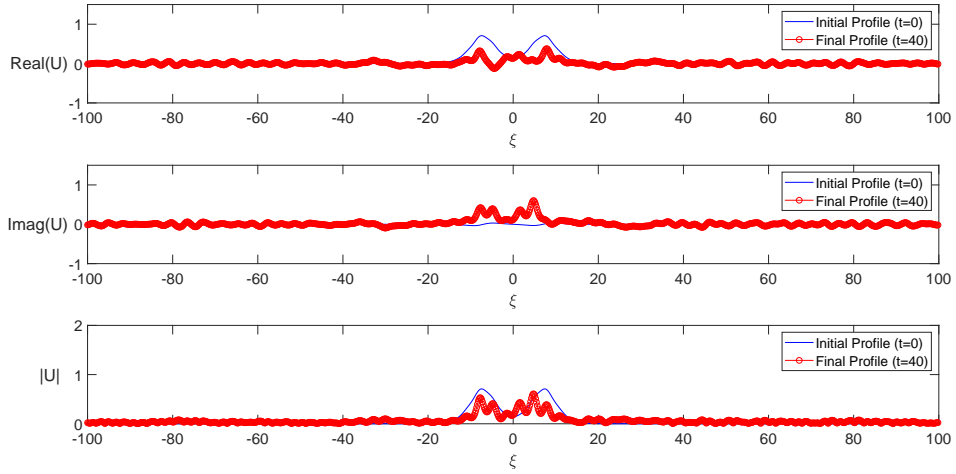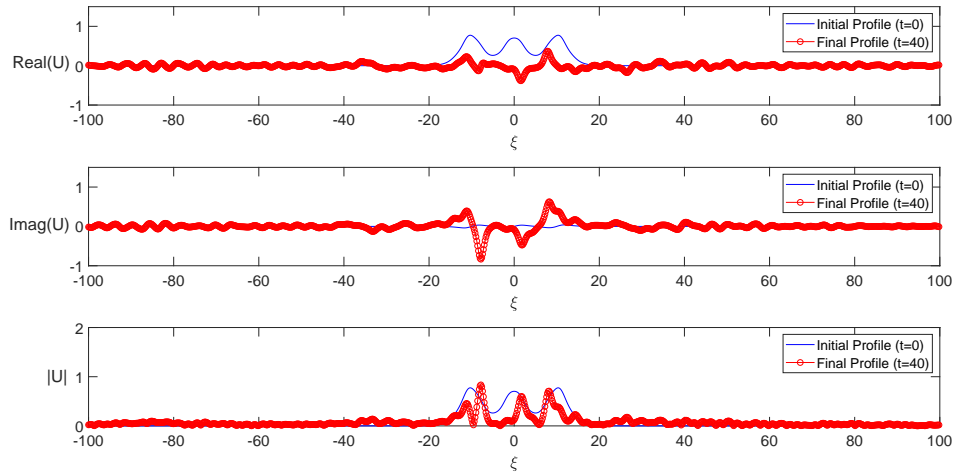


Figure 5.67: Self-localized three soliton solution at two different times $t = 0$ and $t = 40$ for $\mu_3 = 0.002$ with photorefractive potential; a) Real part of U, b) Imaginary part of U, c) Absolute value of U.

# Chapter 6

# Conclusion

In this thesis, we performed an analytical and numerical analysis of the dissipative Kundu-Eckhaus equation. Firstly, we have derived an analytical solution of the dissipative Kundu-Eckhaus equation in the form of a simple monochromatic sinusoid. Then, we have developed a split step Fourier method for its numerical solution and checked the accuracy and the stability of the numerical scheme employing the analytical solution as a benchmark problem. After checking the accuracy and the stability of the scheme, we investigated the rogue wave dynamics of the dissipative Kundu-Eckhaus equation numerically. Our analysis clearly showed that large amplitude fluctuations with an unexpected behavior can be observed in the frame of the dissipative Kundu-Eckhaus equation. Following the vast majority of literature, it is possible to name these fluctuations of the dissipative Kundu-Eckhaus equation as rogue waves. We have analyzed the effects the various coefficients of dissipative Kundu-Eckhaus equation and a photorefractive potential term on such rogue waves. More specifically, we have presented the probability distribution functions of the chaotic wave field generated in the frame of the dissipative Kundu-Eckhaus equation and showed that the statistics of rogue waves significantly depend on the parameters used in the computations and the coefficients of the dissipative Kundu-Eckhaus equation. Among our findings, we observed that the probability distributions exhibit an increase for larger amplitudes when the modulation instability parameters $\beta$ and $m$ increase. Additionally, we have also observed that the photorefractive potential term leads to

generation of waves with larger amplitudes which causes a rightward shift in the peaks of probability distribution functions. However, the parameter having the most dominant effect of amplitude probability distribution turned out to be the dissipation parameter. We have observed that even a small dissipation parameter of $\mu_3 = 0.1$ can destroy the appearance of rogue waves in the frame of the dissipative Kundu-Eckhaus equation.

Secondly, we have also investigated the self-localized solitons of the dissipative Kundu-Eckhaus equation. For this purpose, we have proposed a Petviashvili method scheme for its numerical solution which can be a used the construct the self-localized solitons starting from arbitrary initial conditions in the form of Gaussians. Again, we have discussed the effects of coefficients of the dissipative Kundu-Eckhaus equation on the properties of such self-localized solitons. We have constructed single, two and three soliton solutions of the dissipative Kundu-Eckhaus equation by using the Petviashvili method scheme, therefore, it is possible to conclude that such solitons exist under the effect of no potential as well as the photorefractive potential. Then, we have investigated the stabilities and temporal dynamics of those self-localized solitons. In order to study their temporal dynamics we used the self-localized solitons obtained by the Petviashvili method as initial conditions and subjected them to time integration using the split step Fourier method. In this thesis, by analyzing the time versus power and time versus peak amplitude graphs, we have showed that a dissipation parameter can be used to stabilize those unstable solitons. We have discussed the temporal dynamics of those solitons under the effect of dissipation and showed that the soliton shapes can be preserved with some distortion for time scales sufficient for many engineering studies.

As discussed in the Introduction of this thesis, the Kundu-Eckhaus equation can be used as a model to investigate various phenomena in hydrodynamics, fiber and nonlinear optics, ion-acoustics medium, plasmas and finance, just to name a few.

It is possible to extend these studies to include the effects of dissipation. Therefore, the dissipative Kundu-Eckhaus equation can be used as a model to investigate the similar phenomena in those branches when the effects of dissipation/gain is important. In hydrodynamics and plasmas, for example, the dissipation/gain term can represent energy loss/gain due to turbulence/momentum transfer into the hydrodynamic medium or plasma. In fiber optics, the dissipation term can represent lossy medium whereas the gain stands for energy pumping into the medium. In finance, the dissipation/gain parameter can be used to model the inflow/outflow of assets and goods into/out of the market. Therefore, our findings on the dissipative Kundu-Eckhaus equation can be used the model rogue wave phenomena and the existence, stability and interaction of self-localized solitons in these studies.

In near future, our results can shed light upon many different research activities. The analysis on the effects of dissipation adopted in this thesis can be easily extended to other types of equations in nonlinear Schrödinger class. Some possibilities are to investigate the effects of dissipation on various phenomena modeled in the frame of nonlinear Schrödinger with self-steepening and higher order dispersion and nonlinear terms, Dysthe, Sasa-Satsuma, Kodama-Hassegawa and other equations in the nonlinear Schrödinger class not necessarily restricted to 1D. Additionally, the effects dissipation under various types of potentials can also be studied in the frame of the methodology of this thesis. The potential function can include saturable nonlinearity terms, or it can be extended to other forms such as the trapping-well potential for the quantum simple harmonic oscillator and to photonic graphene potential to study the dissipative dynamics in those fields.

# References

[1] D. Y. Gao and F. Zhaosheng, "A nonconvex dissipative system and its applications (2)," *Journal Global of Optimization*, vol. 4, no. 40, pp. 637–651, 2008.

[2] M. Shehata, "Exact travelling wave solutions for nonlinear evolution equation," *Journal of Computational and Theoratical Nanoscience*, vol. 13, pp. 534–538, 2016.

[3] D. Levi and C. Scimiterna, "The Kundu-Eckhaus and its discretizations," *Journal of Physics a Mathematical and Theoretical*, vol. 42, no. 465203, p. 8, 2009.

[4] A. Kundu, "Landau Lifshitz and higher-order nonlinear systems gauge generated from nonlinear Schrödinger-type equations," *Journal of Mathematical Physics*, vol. 25, 1984.

[5] W. Eckhaus, "The long-time behaviour for perturbed wave-equations and related problems," *Trends in Applications of Pure Mathematics to Mechanics*, no. 404, 1985.

[6] B. A. Molamed, "Evolution of nonsolution and quasi classical wavetrains in nonlinear Schrödinger equation and Korteweg de Vries equation with dissipative perturbation," *Physica D*, no. 29, pp. 155–172, 1987.

[7] M. Lighthill, "Contributions to the theory of waves in non-linear dispersive systems," *Journal of the Institute of Mathematics and its Applications*, vol. 1, pp. 269–306, 1965.

[8] D. Griffiths, "Schrödinger equation," in *Introduction to quantum mechanics*, ser. CVPR '13.  Newyork, USA: Pearson Prentice Hall, 1992, pp. 1–28.

[9] T. Benjamin and J. Feir, "The disintegration of wave trains on deep water," *Journal of Fluid Mechanics*, vol. 27, pp. 417–430, 1967.

[10] J. Weideman and M. Herbst, "Instability of periodic wavetrains in nonlinear dispersive systems," *Proceedings of the Royal Society; a Mathematical, Physical and Engineering Sciences*, vol. 299, p. 5975, 1967.

[11] A. Dyachenko and V. Zakharov, "Modulation instability of stokes wave- freak wave," *JETP Letters*, vol. 81, no. 6, pp. 255–259, 2005.

[12] L. Ostrovsky and V. Zakharov, "Modulation instability: The beginning," *Physica D*, vol. 238, pp. 540–548, 2009.

[13] N. Akhmediev and V. Korneev, "Modulation instability and periodic solutions of the nonlinear Schrödinger equation," *Teoreticheskaya i Matematicheskaya Fizika,*, vol. 69, no. 2, pp. 189–194, 1986.

[14] K. Dysthe, "Note on a modification to the nonlinear Schrödinger equation for application to deep water waves," *Proceedings of the Royal Society; a Mathematical, Physical and Engineering Sciences*, vol. 369, no. 105, 1979.

[15] L. Ostrovskii, "Propagation of wave packets and spacetime self-focusing in a nonlinear medium," *Journal of Experimental and Theoretical Physics*, vol. 24, p. 797800, 1967.

[16] L. Ostrovskii and L. Soustov, "Self-modulation of electromagnetic waves in nonlinear transmission lines," *Izvestiya VUZ, Radiofizika*, vol. 15, p. 242248, 1972.

[17] M. Toomanian and N. Asadi, "Reduction for Kundu-Eckhaus equation via lie symmetric analysis," *Mathematical Science*, vol. 7, no. 50, pp. 1–4, 2013.

[18] A. G. İzergin and E. Korepin, "A lattice model related to the nonlinear schroedinger equation," *Doklady Akademii Nauk*, vol. 259, p. 76, 1981.

[19] S. Hossain, M. Akbar, and A. Wazwaz, "Closed from solutions of complex wave equation via the modified simple equation method," *Cogent Physics*, vol. 4, no. 1, pp. 1–11, 2017.

[20] M. İnc, I. Aliyu, A. Yusuf, and D. Baleonu, "Dispersive optical solution and modulation instability analysis of Schrödinger-Hirota equation with spatio-temporal dispersion Kerr law nonlinearity," *Superlattices and Microstructures*, vol. 113, pp. 319–327, 2017.

[21] C. Liu, Y. Li, M. Gao, Z. Wang, Z. Dai, and C. J. Wang, "Rogue waves solutions of the nonlinear Schrödinger equation with variable coefficient," *Journal of Physics*, vol. 6, no. 85, pp. 1063–1072, 2015.

[22] K. Nozaki and N. Bekki, "Soliton as attractors of a forced dissipative nonlinear Schrödinger equation," *Physics Letters A*, vol. 102A, no. 9, pp. 383–386, 1984.

[23] F. Abdullaev, V. Konotop, M. Solerno, and A. Yulin, "Dissipative periodic waves, solitons and breathers of the nonlinear Schrödinger equation complex potentials," *Physical Review E*, vol. 82, no. 056606, pp. 135–142, 2010.

[24] S. H. Chen, F. Baronio, J. M. Soto, Y. Liu, and P. Grelu, "Chirped Peregrine solitons in a class of cubic-quintic nonlinear Schrödinger equation ," *Physical Review E*, vol. 93, no. 6, 2016.

[25] H. Demiray, "A note on the exact travelling wave solution to the KdV Burgers equation," *Wave motion*, vol. 38, no. 4, pp. 367–369, 2003.

[26] P. Clarkson and C. Cosgrove, "Painleve analysis of the nonlinear Schrödinger family of equations," *Journal of Physics*, vol. 8, no. 20, p. 16, 2003.

[27] P. Clarkson and J. Tuszynski, "Exact multisoliton solution general nonlinear Schrödinger equation with derivative ," *Journal of Physics A: Mathematical and General*, vol. 23, no. 19, pp. 4269–4288, 1990.

[28] R. Conte, "The Painleve approach to nonlinear ordinary differantial equation," *CRM Series in Mathematical Physics*, no. 9710020, pp. 97–103, 1997.

[29] L. Li and F. Yu, "Optical discrete rogue waves solution and numerical simulations for coupled Ablowitz Ladik equation with variable coefficient ," *Nonlinear Dynamics*, vol. 91, no. 3, pp. 1993–2005, 2017.

[30] H. Baskonus, "New complex and hyperbolic function solution to the generalized doubled combined sinh-cosh-Gordon," *AIP Conference Proceedings*, vol. 1798, no. 020018, 2017.

[31] X. Y. Gao, "Variety of the cosmic plasmas: general variable coefficint Kudryashov de Vries-Burgers equation with experimental observational support," *A Letter Journal Exploring the Frontiers of Physics*, vol. 110, no. 1, 2015.

[32] E. Aslan, F. Tchier, and M. İnc, "On optical solutions of the Schrödinger-Hirota equation with power law non-linearity optical fiber," *Superlattices and Microstructers*, vol. 105, no. 0749, pp. 48–55, 2017.

[33] X. Geng and H. Tam, "Darboux transformation and soliton solutions for generalized nonlinear Schrödinger equation," *Journal of the Physical Society of Japan*, vol. 68, no. 5, pp. 1508–1512, 1999.

[34] N. Kudryashov, "A note on the G'/G expansion method," *Applied Mathematics and Computation*, vol. 217, no. 4, pp. 1755–1758, 2010.

[35] G. Xu, "Extended auxiliary equation method and its application to three generalized nonlinear Schrödinger equation," *Abstract and Applied Analysis*, no. Article ID: 541370, p. 8 pp, 2014.

[36] N. Hayashi, E. Kaikina, and P. Naumkin, "Long time behaviour of solutions to the dissipative nonlinear Schrödinger equation," *Proceedings of the Royal Society of Edinburgh*, vol. 130, no. 5, pp. 1029–1043, 2000.

[37] D. Schuch, K. Chung, and H. Hartmann, "Nonlinear Schrödinger type field equation for the description of dissipative systems 1. derivation of the nonlinear field equation and dimensional example," *Journal of Mathematical Physics*, vol. 24, no. 6, pp. 1652–1660, 1983.

[38] V. Bareshenkov, M. Bogdan, and V. Karabov, "Stability diagram of the phase-locked solitons in the parametrically drives, damped,nonlinear Schrödinger equation," *Europhysics Letters*, vol. 15, no. 2, pp. 113–118, 1991.

[39] G. Haller and S. Wiggins, "Multi-pulse jumping orbits and homoclinic treats in a modal truncation of the damped forced nonlinear Schrödinger equation," *Physica D*, no. 85, pp. 311–347, 1995.

[40] H. Demiray, "An analytical solution to the dissipative nonlinear Schrödinger equation," *Applied Mathematics and Computation*, vol. 145, pp. 179–184, 2003.

[41] C. Bayındır, "Analytical and numerical aspects of the dissipative nonlinear Schrödinger equation," *TWMS Journal of Applied and Engineering Mathematics*, no. 6, pp. 135–142, 2016.

[42] A. Kundu and W. Stramppp, "Derivative and higher order extensions of Dawey-Stewartson equation from matrix KadomtsevPetviashvili hierarchy," *Journal of Mathematical Physics*, vol. 36, no. 8, pp. 4192–4202, 1995.

[43] A. Kundu, "Quantum integrable systems construction solution algebraic aspect," *Arxiv Preprint*, no. arXiv:9612046v1, pp. 61–130, 1996.

[44] A. Kundu, "Quantum integrable Systems: basic concepts and brief overview," *ArXiv Preprinted*, no. arXiv:9708114, p. 16, 1997.

[45] X. Wang, B. Tian, Y. Chen, and Y. Yang, "Higher-order rogue wave solutions of the Kundu-Eckhaus equation," *Physica Scripta*, vol. 89, no. 095210, p. 15, 2014.

[46] M. Khater, A. Seadawy, and D. Lu, "Optical soliton and rogue waves solution of the ultrashort femto second pulses in an optical fiber via two different methods and its application," *International Journal for Light and Electron Optics*, vol. 158, pp. 434–450, 2018.

[47] C. Bayındır, "Rogue waves of the Kundu-Eckhaus equation in a chaotic wave field," *Physical Review E*, vol. 93, no. 032201, 2016.

[48] C. Bayındır, "Rogue wave spectra of the Kundu-Eckhaus equation," *Physical Review E*, vol. 93, no. 062215, 2016.

[49] C. Bayındır, "An extended Kundu-Eckhaus equation for modeling dynamics of rogue waves in a chaotic wave current field," *Proceeding of the 12th International Congress of Advances in Civil Engineering*, no. arXiv:1602.05339, 2016.

[50] X. Xi-Yang, B. Tian, W. Sun, and Y. Sun, "Rogue waves solutions for the Kundu-Eckhaus equation with variable coefficient in an optical fiber," *Nonlinear Dynamics*, vol. 81, no. 3, pp. 1349–1354, 2015.

[51] A. Biswas, S. Arshed, M. Ekici, Q. Zhou, S. Moshokoa, A. M., and M. Belic, "Optical soliton solution in briefringent fiber with Kundu-Eckhaus equation," *International Journal for Light and Electron Optics*, vol. 178, pp. 550–556, 2018.

[52] C. Bayındır, "Self-localized solutions of the Kundu-Eckhaus equation in nonlinear waveguides," *Results in Physics*, vol. 14, no. 102362, 2019.

[53] R. Conte and M. Musette, "Exact solution to the partially integrable Eckhaus equation," *Theoretical and Mathematical Physics*, vol. 99, no. 2, pp. 543–548, 1994.

[54] H. Baskonus and H. Bulut, "On the complex structures of Kundu-Eckhaus equation via improved Bernoulli sub-equation function method," *Waves in Random and Complex Media*, vol. 25, no. 4, pp. 720–728, 2015.

[55] O. Gaxiola, "The Laplace-Adomian decomposition method applied to the Kundu-Eckhaus equation," *Arxiv Preprint*, no. arXiv:1704.07730v1, p. 13, 2017.

[56] B. Guo and N. Liu, "Initial boundary value problem and long time asymptotic for the Kundu-Eckhaus equation on the half line," *Mathematical Applied*, vol. 53, no. 061505, p. 32, 2017.

[57] B. Guo and N. Liu, "Long-time asymptotic for the Kundu-Eckhaus equation on the half line," *Journal of Mathematical Physics*, vol. 59, no. 061505, p. 20, 2018.

[58] D. S. Wang and X. Wang, "Long-time asymptotics and the bright n-soliton solutions of the KunduEckhaus equation via the RiemannHilbert approach," *Nonlinear Analysis: Real World Applications*, vol. 41, pp. 334–361, 2018.

[59] S. Arshed, M. Biswas, A. Abdelaty, and Q. Zhou, "Optical soliton perturbation with Kundu-Eckahus equation by $\exp \phi(\xi)$ expansion scheme and $G'/G^2$ expansion method," *International Journal for Light and Electron Optics*, vol. 172, pp. 79–85, 2018.

[60] W. Ping, L. Feng, L. Guo, and T. Shang, "Analytical soliton solution for the cubic-quintic nonlinear Schrödinger equation with Raman effect in nonuniform management systems," *Nonlinear Dynamics*, vol. 79, no. 1, pp. 387–395, 2015.

[61] M. Ekici, M. Mirzazadeh, A. Sonmezoglu, Z. Qin, A. Moshokoa, Seithuti P.and Biswas, and M. Belic, "Dark and singular optical solitons with Kundu-Eckhaus equation by extended trial equation method and extended G'/G expansion scheme," *International Journal for Light and Electron Optics*, vol. 127, no. 22, pp. 10 490–10 497, 2016.

[62] Y. Yong, X. Wang, and T. Yan, "Optical temporal rogue waves in the generalized inhomogenous nonlinear Schrödinger equation with varying higher-order even and odd terms," *Nonlinear Dynamics*, vol. 81, pp. 833–842, 2015.

[63] A. Chabhoub, N. Hoffmann, and N. Akhmediev, "Rogue wave observation in a water wave tank," *Physical Review Letters*, vol. 106, no. 204502, 2011.

[64] Y. Ohta and J. Yang, "Dynamics of rogue waves in the Davey-Stewartson 2 equation," *Journal of Physics a Mathematical and Theoretical*, vol. 46, no. 105202, p. 19, 2013.

[65] M. İnc, A. Aliyu, A. Yusuf, and D. Baleanu, "Gray optical soliton linear stability analysis and conservation laws via multipliers to the cubic nonlinear Schrödinger," *International Journal for Light and Electron Optics*, vol. 164, pp. 472–478, 2018.

[66] D. Pathria and J. Morris, "Pseudo-spectral solution of nonlinear Schrödinger equation," *Journal of Computational Physics*, vol. 87, pp. 108–125, 1990.

[67] G. Dockery and J. Kuttler, "An improved impedance-boundary algorithm for Fourier split-step method of the parabolic wave equation," *IEEE Transaction on antennas and propagation*, vol. 44, no. 12, pp. 51 592–1599, 1996.

[68] M. Dehghan and A. Taleei, "A compact split-step finite difference method for solving the nonlinear Schrödinger equation with constant and variable coefficient," *Computer Physics Communications*, vol. 181, pp. 43–51, 2010.

[69] R. Holzloner, J. Zweck, V. Inkin, and C. Menyuk, "Optimization of the split-step fourier method in modeling optical fiber communications systems," *Journal of Lightwave Technology*, vol. 21, no. 1, 2003.

[70] J. Weideman and M. Herbst, "Split-step methods for the solution of the nonlinear Schrödinger equation," *Society for Industrial and Applied Mathematics*, vol. 23, no. 4, pp. 485–507, 1986.

[71] R. Freire, P. Stoffa, J. Fokkemat, and P. Kessinger, "Split-step fourier migration," *Geophysics*, vol. 55, no. 4, pp. 410–421, 1990.

[72] Y. Bogomolov and A. Yunakovsky, "Split-step Fourier methods for nonlinear Schrödinger equation," *Days of Diffraction*, pp. 34–43, 2006.

[73] V. I. Petviashvili, "Equation of an extraordinary soliton," *Journal of Experimental and Theoretical Physics*, vol. 2, no. 257, 1976.

[74] Z. Musslimani and J. Ablowitz, "Spectral renormalization method for computing self-localized solutions to nonlinear systems," *Optics Letters*, vol. 30, no. 16, pp. 2140–2142, 2005.

[75] J. Fröhlich, M. Griesemer, and I. Sigal, "Spectral renormalization group," *arXiv preprint*, no. arXiv: 0811.2616v1, 2008.

[76] N. Antar, "Pseudospectral renormalization method for solitons in quasicrystal lattice with the cubic-quintic nonlinearity," *Hindawi Publishing Corporation Journal of Applied Mathematics*, vol. 2014, no. 848153, p. 17, 2014.

[77] Z. Musslimani and J. Cole, "Time dependent spectral renormalization method," *Preprint submitted to Physica D*, no. arXiv:1702.06851, 2017.

[78] C. Bayındır, "Self-localized solutions of the Kundu-Eckhaus equation in nonlinearwaveguides," *Results in Physics*, vol. 14, no. 102362, 2019.

[79] M. I. Weinstein, "Modulational stability of ground states of nonlinear schrdinger equations," *SIAM Journal on Mathematical Analysis*, vol. 16, no. 472, 1985.

[80] Y. Sivan, G. Fibich, B. Ilan, and M. I. Weinstein, "Qualitative and quantitative analysis of stability and instability dynamics of positive lattice solitons," *Physical Review E*, vol. 78, no. 046602, 2008.

[81] N. Vakhitov and A. Kolokolov, "Stationary solutions of the wave equation in a medium with nonlinearity saturation," *Radiophysics and Quantum Electronics*, vol. 16, no. 783, 1973.